

Evaluation of Mitochondrial Dysfunction and α -Synuclein Aggregation in Yeast Models of Parkinson's Disease

Michael Zorniak*

Department of Biology
Lake Forest College
Lake Forest, Illinois 60045

Summary

Parkinson's disease (PD) is characterized by the progressive death of dopaminergic neurons in the human brain. The misfolding and aggregation of α -synuclein, as well as the presence of reactive oxygen species (ROS), are thought to contribute to this cytotoxicity. The mechanism of interaction between these two pathways is unknown. Mitochondrial dysfunction, specifically, incomplete respiratory metabolism and loss of antioxidants, has long been implicated as the culprit for ROS accumulation. Our lab has previously developed budding and fission yeast models to study genetic regulation of α -synuclein misfolding and toxicity. My thesis is composed of two studies. For my first goal, I tested the hypothesis that a mitochondrial dysfunction would enhance α -synuclein misfolding, aggregation, and toxicity. I used two budding yeast strains, one knocked-out for α -ketoglutarate dehydrogenase (the respiratory mutant) and mitochondrial glyoxalase II (the anti-oxidant mutant) to study the combinatorial effects of oxidative stress and expression of human α -synuclein. We found no cellular toxicity and decreased α -synuclein expression in both strains, yet intracellular aggregates only in the respiratory mutant. For my second goal, I tested the hypothesis that changing key amino acids within α -synuclein would affect its folding and toxic properties. Specifically, I investigated a mathematically modeled mutation of α -synuclein, Ala⁷⁶→Glu, which is thought to change its shape in a way that decreases its rate of aggregation. In fission yeast, A76E- α -synuclein formed aggregates more slowly than the normal form and did not change toxicity or expression. In budding yeast, A76E- α -synuclein reached the membrane more slowly, initially had decreased expression, and exhibited no toxicity. Results from these two studies assert that mitochondrial dysfunction and α -synuclein shapes play a role in the manifestation of Parkinson's disease.

Introduction

Neurodegeneration is characterized by the progressive death of neurons in the central nervous system leading to an array of dementias and motor dysfunctions. The past decade has witnessed rapid convergence in the study of neurodegenerative diseases (NDD; Figure 1). Scientists immersed in the evaluation of Alzheimer's disease (AD), Huntington's disease, transmissible spongiform encephalopathies, Parkinson's disease (PD), and many other NDD are coming

together and finding common disease-causing pathways (Muchowski 2002). As a result, scientists studying NDD are asking the same questions about their respective discipline. Their questions are so similar that they can be applied to virtually any NDD model. Moreover, within each NDD, seemingly unrelated disease-causing pathways are being linked together.

Principally, neurodegeneration is pathologically highlighted by proteinaceous deposits in and around dying neurons. To that end, key proteins have been identified as culprits for each NDD. Familial forms of NDD generally come from a mutation in that protein. However, most NDD are recorded as sporadic events where the protein acquires a different shape due to a mutation, post-translational modification, inactivity of a chaperone, or even the interaction with an infectious protein (i.e. prions; Ellis *et al.*, 2002). For instance, in Alzheimer's disease, A β amyloid is found in extracellular aggregates (Caughey *et al.*, 2003). Consequently, this key protein typically attains an anti-parallel β -sheet conformation, which ultimately self-assembles to form fibrils and then aggregates—a common pathological feature among NDD. Scientists have yet to discover whether or not insoluble protein aggregates are neuroprotective or cytotoxic. Some now argue that the soluble pre-fibrillar intermediates—protofibrils—are the key toxic microelements (Caughey *et al.*, 2003). Furthermore, intense research is attempting to unravel the toxic elements in NDD, which is being progressively combined with pathways in mitochondrial dysfunction and oxidative stress in NDD.

Aging, and its deleterious effects on the organism, is partly due to the cell's inability to regulate its redox status. Accumulating evidence suggests that mitochondrial dysfunction and oxidative stress are key factors in the onset and development of NDD (Dauer *et al.*, 2003). Oxidative stress is the accumulation of reactive oxygen species (ROS), which has been recently evaluated as a unifying factor in PD pathogenesis (Abou-Sleiman *et al.*, 2006). Non-dividing neurons in the human brain are especially sensitive to oxidative stress because their longevity allows for the progressive buildup of oxidatively modified DNA, proteins, and lipids.

The aggregation of misfolded proteins and mitochondrial dysfunction are not mutually exclusive. Research has only recently been able to make ties between each respective theory as a result of genetic screens (Clark *et al.*, 2006). By studying the cellular events that cause PD, we may be able to elucidate the mechanism by which proteins misfold in all NDD.

Unfortunately, the toxic molecules responsible for PD still remain to be resolved (Dauer *et al.*, 2003). α -Synuclein, the protein that misfolds in PD, forms aggregates that may be toxic or protective to the cell (Caughey *et al.*, 2003). Combined with accumulating ROS, the disease-causing agent remains to be determined. My thesis is divided into two studies which involves the understanding of two questions. How does mitochondrial dysfunction contribute to α -synuclein misfolding and toxicity? And, how does

*This author wrote the paper as a Senior thesis under the direction of Dr. Shubhik DebBurman.

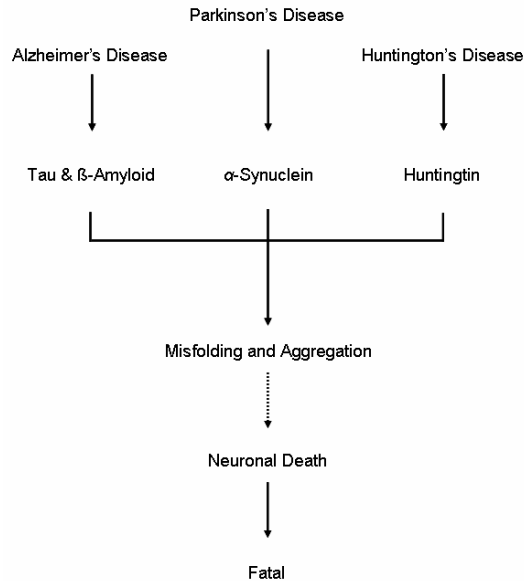


Figure 1. Protein Misfolding is a Common Theme in Neurodegenerative Diseases. All progressively fatal neurodegenerative diseases are associated with the misfolding of a key protein. The aggregation of these proteins is hypothesized to cause cell death in the brains of patients with the above diseases. Due to their mechanistic unity, the elucidation of one disease pathway may allow for the understanding of the others. The dotted line indicates a correlation and not a linear causal relationship.

altering the shape of α -synuclein contribute to its rate of aggregation and toxicity?

The following subsections will highlight the mechanisms behind mitochondrial dysfunction and α -synuclein aggregation in PD. I will then provide my thesis hypotheses, aims, and experimental design.

Parkinson's Disease

Nearly 500,000 people are afflicted with PD in the United States, making it the second most prevalent neurodegenerative disease after AD (Caughey *et al.*, 2003). Neuronal death in PD specifically occurs in dopaminergic neurons of the substantia nigra *pars compacta* (SNpc). The progressive development of cytoplasmic inclusions, known as "Lewy bodies" (LB), in the SNpc is correlated with cell death (Spillantini *et al.*, 1998). LB are predominantly composed of α -synuclein, a cytosolic protein of unknown function. Additionally, extensive neurodegeneration and LB presence is observed in non-dopaminergic systems in PD: locus coeruleus, raphe, cerebral cortex, and olfactory bulbs (Dauer *et al.*, 2003).

Patients with PD generally experience postural rigidity, resting tremors, and slowness of movement (Goedert *et al.*, 2001). Clinical manifestations of PD are due to striatal scarcities in dopamine, which can be abated by replenishing dopamine concentrations with the precursor levodopa (L-3,4-dihydroxyphenylalanine; Dauer *et al.*, 2003). Interestingly, positron emission tomography (PET) imaging can be used to measure dopamine synthesis and transport to detect presymptomatic stages of the disease (Elsinga *et al.*, 2006). The development of PET detection of PD has reemphasized the utility of PD vaccination with α -synuclein antibodies—currently in clinical trials (Pilcher 2005)—before symptoms arise in

diagnosed patients (May *et al.*, 2006). A step toward α -synuclein toxicity is its localization to the plasma membrane of substantia nigral cells (Masliah *et al.*, 2005). Thus, α -synuclein antibodies have been implicated as a promising preventative treatment due to the antibodies' ability to neutralize toxic α -synuclein bound to the outside membrane.

Parkinson's disease is 95% idiopathic; yet, accumulating evidence suggests familial and environmental links to PD. New familial links to PD are α -synuclein-centric autosomal-dominant mutations (Hofer *et al.*, 2004). In 1997, Contursi and colleagues reported an A53T missense mutation in the α -synuclein gene of a Greek family. The following year, an A30P mutation was coupled with early-onset PD in a German family (Krueger *et al.*, 2001). Then in 2004, a Spanish family was found to have an E46K mutation, within a conserved region of α -synuclein, which displayed classical PD pathology with Lewy body dementia (Zarranz *et al.*, 2004). These developments demonstrate a genetic connection to PD. Newly discovered autosomal-recessive genes, with the exception of LRRK2 which is autosomal-dominant (Paisan-Ruiz *et al.*, 2004; Zimprich *et al.*, 2004), have been identified and intimately tied to α -synuclein-dependent toxicity: UCH-L1 (Funayama *et al.*, 2002), Parkin (Kitada *et al.*, 1998), DJ-1 (Bonifati *et al.*, 2003), and PINK1 (Valente *et al.*, 2004). These autosomal-recessive genes, when deficient, cause PD without LB pathology.

Pharmacological Evidence for Mitochondrial Dysfunction in Parkinson's Disease

Not only can PD be caused by familial mutations, but chemical agents can be used to create PD-like symptoms. An environmental toxin based model of PD established itself in 1983 by Langston and colleagues. The environmental toxin 1-methyl-4-phenyl-1,2,5,6-tetrahydropyridine (MPTP) caused acute and irreversible damage to the SNpc without LB. MPTP-dependent parkinsonism was challenged with levodopa treatment, which equivalently rescued symptoms when compared to PD patients. Other recently discovered environmental toxins, such as paraquat and rotenone cause less acute dopaminergic degeneration but form α -synuclein dominant LB structures (Dauer *et al.*, 2003). Consequently, all three toxins inhibit mitochondrial complex I activity, which generates rapid generation of ROS, decreased ATP production, and increased intracellular calcium, thereby causing excitotoxic-related cell damage (Abou-Sleiman *et al.*, 2006). Therefore, the ongoing investigation of PD pathogenesis has uncovered two distinct pathways, but only loose relationships between them (Figure 2).

Genetic Evidence for Mitochondrial Dysfunction in Parkinson's Disease

Pedigrees of families with PD have given scientists unique insight into its genetic basis. Among the newly discovered autosomal-recessive Parkinson's disease-linked genes, PINK1 and parkin give us a way to link mitochondrial dysfunction with the ubiquitin proteasome system, thus combining two disparate disease-causing pathways into one schematic (Figure 2; Park *et al.*, 2006; Clark *et al.*, 2006; Yang *et al.*, 2006; Wang *et al.*, 2006).

The parkin gene has been implicated in a form of recessive parkinsonism. Ironically, its

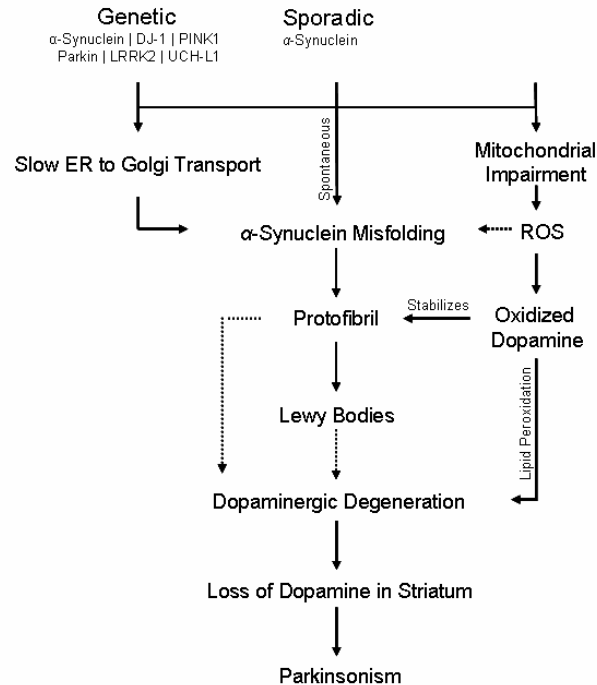


Figure 2. The Role of α -Synuclein and Mitochondrial Dysfunction in Parkinson's Disease. Sporadic, genetic, and environmental factors lead to Parkinson's disease pathogenesis. Emerging evidence suggests that these three factors can interact and synergistically affect α -synuclein folding. The pathways illustrated above shows α -synuclein at the center. Yet, environmental toxins, such as MPTP, lead to dopaminergic degeneration without Lewy body inclusions or α -synuclein-rich aggregates. The dotted pathways indicate that the main toxic agent, either protofibrils or Lewy bodies, remains to be determined (Conway *et al.*, 2001).

phenotype is devoid of LB, pathology similar to MPTP exposure (Cookson *et al.*, 2005). This suggests that LB are not needed for PD to occur. Parkin codes for a ligase that tags damaged or misfolded proteins with ubiquitin (Cookson *et al.*, 2005). The tagged proteins are then recycled in the proteasome. PINK1 is structurally and functionally different from parkin, but is also implicated in a recessive form of PD. It encodes a kinase that localizes to the intermembrane space of mitochondria (Abeliovich *et al.*, 2006). Yet, the question remains, how do these different proteins contribute to our understanding of PD?

Park *et al.* (2006) and Clark *et al.* (2006) have shown that knock-out mutants for parkin and PINK1 are the key to understanding their purpose in PD pathogenesis. When PINK1 was removed from the flies (i.e. *Drosophila melanogaster*), dopaminergic degeneration with motor defects were observed (Park *et al.* 2006). Thus, a dysfunctional mitochondria, due to PINK1 deletion, created a parkinsonian phenotype in flies. Interestingly, the PINK1 mutant phenotype was found to be nearly identical to the parkin mutant (Park *et al.*, 2006). This similarity between both fly strains generated curiosity about how these two proteins may interact.

In a novel experiment, Park and colleagues (2006) overexpressed parkin in a PINK1 mutant. Surprisingly, energy production was recovered. They concluded that parkin is protective against mitochondrial dysfunction. Inversely, PINK1 overexpression in a parkin mutant showed no rescue effect. Therefore, Park *et al.* (2006) along with Clark *et al.* (2006) and Yang *et al.* (2006) concluded that parkin functions downstream of PINK1—a single linear

pathway between the mitochondria and ubiquitin proteasome system.

These insights into the biology of Parkinson's disease have intimately tied mitochondrial dysfunction and the UPS in a programmed cell-death model of PD. Mitochondrial dysfunction can be induced in other ways to generate PD-like pathology.

Cell Death Modulators in the Midbrain

Oxidative stress may play a role in substantia nigra specific atrophy (Lin *et al.*, 2006). Oxidative modifications significantly change α -synuclein and dopamine function, which are then found to increase sensitivity of SNpc neuronal degeneration (Galvin *et al.*, 2006). Neuromelanin, with its high iron content, which pigments the SNpc, may provide a necessary oxidative stress mechanism to specifically destroy the SNpc (Zecca *et al.*, 2006). Iron may aggressively catalyze ROS generation from oxygen-containing substrates like hydrogen peroxide (Gerlach *et al.*, 2003; Figure 3). Additionally, mitochondrial dysfunction by inhibition of complex I may act as possible conduit for a mitochondrial-dependent apoptotic pathway (Tatton *et al.*, 2003). Thus, the disparate pathways of cell death, due to oxidative stress, emphasize further understanding of SNpc specific degeneration.

Dopamine auto-oxidation has long been an attractive hypothesis for SNpc selective death due to its endogenous metabolism in the SNpc (Graham 1978). Normal metabolism of dopamine produces hydrogen peroxide and superoxide radicals, which oxidize dopamine to form dopamine ortho-quinone (Dauer *et al.*, 2003), similar in structure to rotenone, a complex I inhibitor and ROS generator. Dopamine ortho-quinone

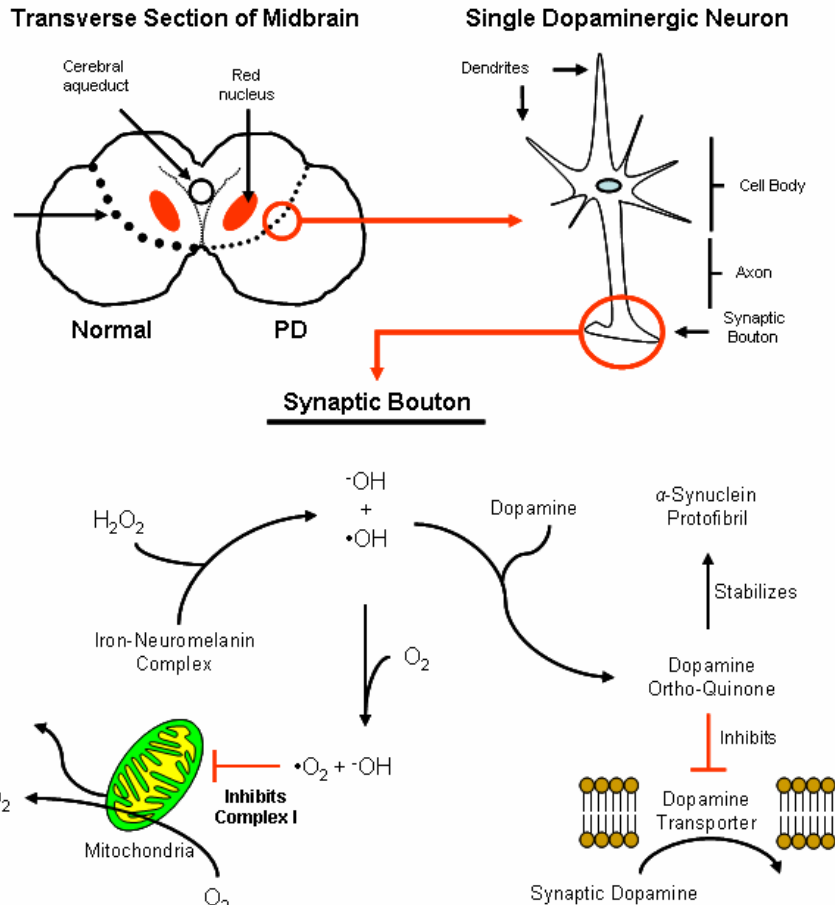


Figure 3. Dopamine Neurons are Specifically Sensitive to ROS. The specific death of substantia nigra neurons in PD is due to toxic relationships between α -synuclein, dopamine, iron-neuromelanin complexes, and ROS. Oxygen radicals can form in two ways: one, hydrogen peroxide and ferrous iron produce a hydroxyl radical and anion, as well as, ferric iron by the Fenton reaction; two, inhibition of complex I in the mitochondria induces singlet oxygen radical production. Dopamine can also become oxidized which can then inhibit the dopamine reuptake transporter and stabilize toxic protofibril aggregate intermediates. Thus, accumulation and generation of oxygen radicals in the substantia nigra is a self-perpetuating process, due to the physical properties of these neurons.

then proceeds to disrupt all proteins with disulfide linkages (Dauer *et al.*, 2003). Auto-oxidation thus has a four-fold effect on the cell (Figure 3). One, the disassembly of proteins with disulfide linkages places an unnecessary stress and load on the ubiquitin-proteasome protein degradation system (UPS; Dauer *et al.*, 2003). Two, ROS generated by dopamine metabolism increases general protein misfolding in the cell, thus further increasing the load onto the UPS. Three, dopamine ortho-quinone, like rotenone, may inhibit mitochondrial complex I activity. And four, dopamine ortho-quinone can inhibit the dopamine transporter on the pre-synaptic bouton, which allows dopamine to stay in the synapse and over activate the post-synaptic membrane, thus having similar effects as cocaine (Whitehead *et al.*, 2003). All of these constituents of dopamine metabolism prime SNpc neurons for self-destruction. Thus, programmed cell-death, induced by ROS and mitochondrial dysfunction, may lead to specific death of SNpc neurons.

α -Ketoglutarate Dehydrogenase Model for PD

With the advent of MPTP studies, the respiratory chain in the mitochondria has been long considered as a major site of ROS generation. Specifically, inhibition of complex I, NADH ubiquinone oxidoreductase, is a

plausible site of ROS production due to its sensitivity to oxidative stress; only 25-30% inhibition of complex I is necessary to induce parkinsonism (Adam-Vizi 2005). Yet, there are other factors that contribute to the toxic redox status in SNpc neurons.

Decreased activity of α -ketoglutarate dehydrogenase (α -KGDH), a regulatory Krebs' cycle enzyme, disrupts the redox status in brains of Parkinson's and Alzheimer's disease patients (Gibson *et al.*, 2000). To gauge its effect, mitochondrial membrane potentiation is used as an indicator of oxidation-reduction reactions taking place within the cell (Gibson *et al.*, 2000). Loss of membrane potentiation leads to an apoptotic state within the cell, as described above. α -KGDH is regulated by the NADH/NAD⁺ ratio, Ca²⁺, and ADP (Adam-Vizi, 2005). Its loss-of-function would thus eliminate a key modulating location in glucose metabolism. Interestingly, the isolated enzyme produces hydrogen peroxide and superoxide radicals *in vitro* (Tretter and Adam-Vizi, 2004). These results were found to hold true *in vivo* as well (Starkov *et al.*, 2004). This generation of ROS was dependent on the NADH/NAD⁺ ratio, where increasing NADH levels account for this phenomenon. Increasing ROS levels actually inhibit α -KGDH (Tretter and Adam-Vizi, 1999). The inhibition of α -KGDH reduces NADH for the

electron transport chain, thus decreasing ATP production. Thus, by these inverse pathways, α -KGDH is both a target and generator of oxidative stress.

Markedly, α -KGDH may regulate complex I activity by these inverse pathways (Adam-Vizi, 2005). As stated before, inhibition of α -KGDH reduces NADH production which kinetically decreases complex I (NADH ubiquinone oxidoreductase) activity. The other inhibitory pathway is set in motion by a high NADH concentration. Thus, complex I is kinetically active under these conditions. The generation of ROS by α -KGDH in the mitochondrial matrix may disrupt complex I activity (Figure 4). Also, the ROS generated by α -KGDH would increase lipid peroxidation thereby disrupting calcium homeostasis. Lipid disruption would furthermore perturb the pH gradient across the inner membrane space. The loss of membrane potentiation is a step towards apoptosis. Loss of α -KGDH activity and inhibition of complex I is a similar to the MPTP-based model of PD.

Loss of α -KGDH activity also occurs in AD. Gibson and colleagues (1988) have demonstrated that α -KGDH activity is reduced by 40-75% in AD brains. Reduction in α -KGDH levels is negatively correlated with neurofibrillary tau tangle counts, suggesting this enzyme is involved in the neurodegenerative cascade. Even 10 to 15% reduction in available glucose or oxygen can reduce brain function, including decline in memory (Gibson *et al.*, 2005). A current study shows how brain regions with low metabolic activity accumulate more plaques in conjunction with dementia (Shoghi-Jadid *et al.*, 2002). The return of glucose to these brain regions reverses some behavioral deficits of AD. This suggests that symptoms in AD are not always attributed to neurodegeneration.

Mitochondrial Glyoxalase II and Neurodegeneration

The maintenance of antioxidants within a cell is the responsibility of a network of proteins, such as catalases, superoxide dismutases, reductases, and peroxidases (Lin *et al.*, 2006). A not so common constituent of this network is the glyoxalase system (Bito *et al.*, 1997). This system is present within many organisms and is thought to be ubiquitous (Bito *et al.*, 1997). The main function of glyoxalases is to detoxify a by-product of glucose metabolism, methylglyoxal (2-oxoaldehyde). The coordination of glyoxalase I and II allow for the complete conversion of this toxic molecule to D-lactate and glutathione (Bito *et al.*, 1999). Glutathione is a major redox molecule and antioxidant which sequesters and inactivates ROS (Drechsel *et al.*, 2007). Thus, the glyoxalase system is both an antioxidant system, because it detoxifies aldehydes, and a generator of antioxidants, glutathione.

The function of the glyoxalase system has been implicated in neurodegenerative diseases. In PD and AD, Lewy Bodies and neurofibrillary tangles are oxidatively modified, resulting in toxic advanced glycation end products (Webster *et al.*, 2005). Among the many reactive carbonyls, methylglyoxal is thought to be the primary substrate for this conversion (Webster *et al.*, 2005). The accumulation of methylglyoxal is correlated with mitochondrial deficiencies and even apoptosis (Xu *et al.*, 2006). A dysfunctional glyoxalase system would have a two-fold deleterious effect. One, methylglyoxal would be more available to oxidatively modify other proteins. Two, the production of glutathione would be inhibited, thus oxidants would have a higher chance of accumulating and damaging cellular structures.

For my first thesis goal, I evaluated the role of mitochondrial dysfunction in PD using a respiratory (α -ketoglutarate dehydrogenase) and antioxidant mutant (mitochondrial glyoxalase II) to study the aggregation and toxicity of α -synuclein.

α -Synuclein's Biological and Pathogenic Properties

The concept of mutant α -synuclein sharing pathogenic pathways with sporadic PD is largely based on α -synuclein-rich LB (Dauer *et al.*, 2003). Yet, the exact cellular function of α -synuclein is unknown.

α -Synuclein is a small, 140 amino acid, 14 kDa, natively unfolded protein found in presynaptic end terminals throughout the entire central nervous system—not just in the SNpc—alongside synaptic vesicles (Kahle *et al.*, 2002). The endogenous location of α -synuclein plays a role in learning, memory, and synaptic plasticity within songbirds (Clayton *et al.*, 1999). α -Synuclein regulates vesicular-trafficking, which may suggest it's role in synaptic plasticity (Jensen *et al.*, 1998). Furthermore, α -synuclein is found lacking a native secondary structure in the cytosol (Weinreb *et al.*, 1996). Strikingly, small acidic lipid vesicles are found attached with an 80% helical- α -synuclein structure (Davidson *et al.*, 1998). α -Synuclein loses its normal function upon lipid binding; this may play a role in neuronal death in PD. The sequestered α -synuclein would seemingly not play an active role in synaptic plasticity, possibly leading to repressed vesicle release. This in turn may cause synaptic connections to degrade due to diminished communication between neurons.

Although α -synuclein's normal function is unknown, properties that allow and protect it from self-assembly have recently been investigated. α -Synuclein is characterized in three sections: N-terminal, central, and C-terminal domains. Interestingly, 11-amino acid variable repeats, XKTKEGVXXXX, exist mainly on the N-terminus (7 conserved repeats), but also on the C-

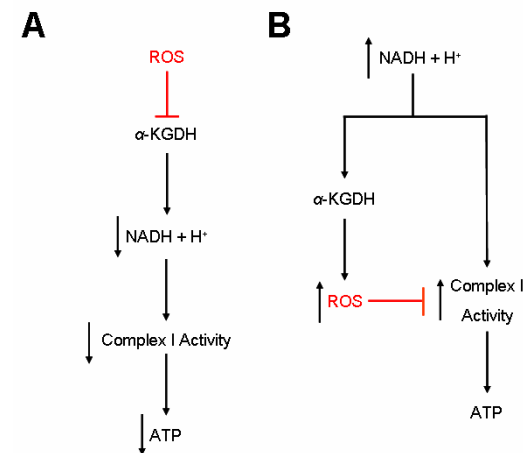


Figure 4. α -KGDH Regulation of Complex I Activity by ROS and NADH Levels. Evidence for the above pathways is adapted from Tretter *et al.* (2004; 2005). The two red perpendicular lines indicate inhibition.

A. *ROS Inhibition of α -KGDH.* ROS inhibits α -KGDH which decreases the production of NADH in the Krebs's cycle. The lack of NADH lowers complex I activity, thus ATP is not synthesized. B. *ROS Generation by α -KGDH.* A high concentration of NADH increases the activity of both α -KGDH and complex I. Yet, this dual activation is counterintuitive. α -KGDH produces ROS when NADH levels are high. This may, in turn, inhibit previously activated complex I.

terminus (only 2; Kessler *et al.*, 2003; Uversky *et al.*, 2002). These regions are found to inhibit the toxic conversion to a β -sheet-rich conformation and thus prevent fibrillization and aggregation. Yet, familial mutations, have been found to increase the rate of fibrillization, A30P slower than A53T (Conway *et al.*, 1998). This suggests that a mutation may induce β -sheet sheet conversion from an unfolded or α -helical state. Soon after, an α -synuclein fibril intermediate was discovered by Conway and colleagues (2001) with atomic force microscopy and hypothesized to be the causative agent in PD. The intermediate was coined the protofibril, which can bind and permeabilize lipid membranes, thereby destroying the integrity of the cell. Whether or not protofibrils or aggregates cause cell-death in PD is still controversial. Shape changes may also affect lipid binding properties of α -synuclein. The binding affinities of A30P and A53T α -synuclein to lipids have been studied previously in our lab (Sharma *et al.*, 2006). Interestingly, E46K and A53T preferentially bound lipids when compared to A30P. A shape change to an α -helical conformation accounts for the enhanced membrane-binding in a synthetic model (Davidson *et al.*, 1998). Further analysis suggests that the C-terminus binds to the membrane, where the N-terminus is unbound (Eliezer *et al.*, 2001).

The variable shape of α -synuclein may account for its acquisition of toxic properties or lack thereof. Chiti and colleagues (2003), mathematically modeled protein aggregation rates as a function of three physicochemical parameters: hydrophobicity, tendency to convert from α -helical to β -sheet conformation, and charge. They suggested that either an A76E or A76R α -synuclein would inhibit aggregation and thus not cause disease. Since most proteins have not been evolutionarily optimized to resist aggregation, the modeled amino acid substitutions may delay the self-assembly of α -synuclein, an aggregation-prone protein (Caughey *et al.*, 2003). Thus, for my second thesis goal, I evaluated the aggregation and toxicity of A76E- α -synuclein and its ability to reduce the rate of fibril formation.

Yeast Model for PD

Our lab has developed budding and fission yeast models of PD to study the genetic regulation of human α -synuclein misfolding and toxicity. *Saccharomyces cerevisiae* (budding yeast) is a powerful genetic system to model protein misfolding processes underlying human diseases (Outeiro and Muchowski, 2004), including prion disease (Ma and Lindquist, 1999), Huntington's disease (Krobitsch and Lindquist, 2000; Muchowski *et al.*, 2000) and amyotrophic lateral sclerosis (Kunst *et al.*, 1997). Recently, three *S. cerevisiae* models for α -synuclein have shed new insight into α -synuclein's pathology and biology (Outeiro and Lindquist, 2003; Dixon *et al.*, 2005; Zabrocki *et al.*, 2005). Additionally, a yeast genetic screen revealed 86 genes that were synthetically lethal with overexpressed α -synuclein (Willingham *et al.*, 2003).

Schizosaccharomyces pombe (fission yeast) is also a powerful model organism in cell biology, providing insight into the eukaryotic cell cycle (Fantès and Beggs, 2000), DNA repair and recombination (Davis and Smith, 2001), and checkpoint controls needed for stability (Humphrey, 2000). Like budding yeast, fission yeast shares with humans a high conservation of protein folding and protein quality control pathways (Wood *et al.*, 2002).

Previous findings in our lab have evaluated the misfolding, aggregation, and toxicity of WT- α -synuclein and three mutants (A30P, A53T, A30P/A53T) in budding yeast when regulated by oxidative stress and proteasomal deficiencies (Sharma *et al.*, 2006). Prominent localization of WT and A53T α -synuclein was found near the plasma membrane. Contrastingly, A30P displayed cytoplasmically diffuse localization compared to a mixed phenotype from A30P/A53T. Within the strains tested, α -synuclein did not contribute to cellular toxicity. In a proteasomal barrel mutant (*doa3-1*), production of α -synuclein was delayed, where in a proteasomal cap mutant (*sen3-1*) α -synuclein aggregation was observed. When cells lacking manganese superoxide dismutase (*sod2*) were challenged with hydrogen peroxide, α -synuclein was extremely lethal. This toxicity was not seen in a copper, zinc superoxide dismutase (*sod1*). No aggregates were seen in *sod2* Δ cells despite the lethality. These experiments support the oligomeric hypothesis as the primary toxic species in PD.

In second study, we used fission yeast to study a different property of α -synuclein misfolding and aggregation (Brandis *et al.*, 2006). Wild-type α -synuclein and three mutants (A30P, A53T, and A30P/A53T) were expressed with vectors of increasing promoter strength to directly test in living cells the nucleation polymerization hypothesis for α -synuclein misfolding and aggregation. In support, A53T formed aggregates in a time- and concentration-dependent manner. Cells expressing A30P/A53T did not exhibit this quality due to cytoplasmic localization of α -synuclein. Wild-type α -synuclein formed aggregates at a slower rate than A53T. Surprisingly, A53T did not localize to the membrane, even at low concentrations allowing for intermediate fibrillization. Toxicity was not observed in all cases tested. Thus, we speculate toxicity is linked to membrane binding capacity.

Budding and fission yeast model different, yet similar properties of α -synuclein pathobiology. For my thesis, I have conducted two studies using both yeasts to understand two separate questions. One, how does mitochondrial dysfunction play a role in PD? Two, can a mutation in α -synuclein change its rate of aggregation?

Study One: Mitochondrial Mutants

Hypothesis: Mitochondrial dysfunction will enhance α -synuclein misfolding, aggregation, and toxicity.

My aim was to evaluate two non-essential mitochondrial budding yeast knockout strains to understand the effect of mitochondrial deficiencies on α -synuclein misfolding and toxicity. Previous studies in our lab suggest that the mitochondria is implicated in α -synuclein toxicity and gave precedence for my evaluation (Sharma *et al.*, 2006). Among the enhancers studied by Willingham and colleagues (2003) I investigated orthologs for α -ketoglutarate dehydrogenase (*kgd1_p*) and mitochondrial glyoxalase II (*gl04_p*), which were knocked-out and found to be sensitive to α -synuclein-induced toxicity. To test this hypothesis, I expressed wild-type and three mutant forms of human α -synuclein tagged in the *kgd1* Δ and *gl04* Δ yeast strains. Data gathered from these experiments was compared to their isogenic parent strain, BY4741, without the specified gene deletions. Additionally, the localization and expression of α -synuclein was evaluated to determine the effects of α -synuclein concentration and position in accordance with cell viability. This analysis allowed us to further characterize which α -synuclein isoform and/or

aggregate intermediate is responsible for cellular toxicity when paired with mitochondrial dysfunction.

Study Two: The A76E α -Synuclein Mutation Hypothesis: The A76E α -synuclein mutation will decrease its rate of aggregation and delay membrane localization.

My aim was to create the A76E α -synuclein mutation and test its localization properties in both budding and fission yeast. In budding yeast, I predicted that A76E α -synuclein would decrease its affinity to bind membranes and cause toxicity through a soluble aggregate intermediate (Figure 5A and 5B). In fission yeast, I predicted that A76E α -synuclein would reduce its aggregation and cause toxicity (Figure 5C and 5D).

To test this hypothesis, I compared A76E- α -synuclein-expressing cells with WT- α -synuclein-expressing cells in BY4741 (budding yeast) and TCP1 (fission yeast). Here, I monitored the fluorescence patterns, toxicity, and expression α -synuclein tagged to GFP. This investigation will aid in our understanding of *in vivo* aggregation kinetics in the pathogenic α -synuclein protein.

Chapter 1: Mitochondrial Mutants Change α -Synuclein Folding and Aggregation

Materials and Methods

Methods adapted from Sharma et al., (2006).

α -Synuclein Expression Vector Constructs.

The pYES2.1/V5-His-TOPO yeast expression vector (Invitrogen) was used for all α -synuclein expression in budding yeast. The following five vector constructs were previously created for each experiment: green fluorescent protein (GFP), wild-type α -synuclein, A30P, A53T, and E46K isoforms of α -synuclein. These mutants were also tagged at the C-terminus with GFP. For all experiments the pYES2.1/V5-His-TOPO vector and the GFP tagged vector were used as expression controls (See Table 1 for List of Constructs)

Yeast Strains.

The parent budding yeast (*Saccharomyces cerevisiae*) strain, BY4741 (*MATa his3 Δ 1 leu2 Δ 0 met15 Δ 0 ura3 Δ 0*) was purchased from Open Biosystems (Huntsville, AL). A respiratory deficient BY4741 strain, knocked out for alpha-ketoglutarate dehydrogenase (*kgd1 Δ*) and glutathione deficient strain, knocked out for mitochondrial glyoxalase II (*glo4 Δ*) was also bought from Open Biosystems.

Yeast Expression.

Expression vectors, containing the *ura3* gene, were transformed into yeast as described in Burke and colleagues (2000). Yeast cells were grown on synthetic-complete media devoid of uracil (SC-URA) to select for transformed cells. Plasmid presence was verified by fluorescence microscopy and polymerase-chain reaction (PCR). A galactose inducible promoter (GAL1), coupled to the pYES2.1 vector, allowed for the regulation of α -synuclein expression. Yeast were first grown overnight in 5 mL of 2% SC-URA glucose media for 12 hours in a shaking-incubator at 30°C. Cells were then diluted to a concentration of 5×10^6 cells/ml and transferred into 2% SC-URA galactose media for induction of GFP and α -synuclein expression. Cell

concentration was obtained by counting using a hemocytometer.

Western Analysis.

A concentration of 2.5×10^7 yeast cells/ml were washed in 50 mM Tris (pH 7.5), 10 mM Na₂S₂O₃ and solubilized in Electrophoresis Sample Buffer (ESB; Burke, 2000) containing 2% sodium dodecyl sulfate (SDS), 80 mM Tris (pH 6.8), 10% glycerol, 1.5% dithiothreitol, 1 mg/ml bromophenol blue, and a cocktail of protease inhibitors and solubilizing agents (1% Triton-X 100, 1 mM phenylmethylsulfonyl fluoride, 1 mM benzamide, 1 mM sodium orthovanadate, 0.7 μ g/ml pepstatin A, 0.5 μ g/ml leupeptin, 10 μ g/ml E64, 2 μ g/ml aprotinin, and 2 μ g/ml chymostatin). Samples were loaded onto 10-20% Tris-Glycine gels (Invitrogen) using Tris-Glycine-SDS running buffer (pH 8.3). Gels were transferred onto PVDF membranes and immunodetection was done with anti-V5 AP monoclonal antibody using standard protocols and detected for alkaline phosphatase activity (NBT/BCIP). A loading control was measured with an anti-PGK monoclonal antibody.

Growth Curve Analysis.

Flasks with 25 ml SC-URA galactose were each inoculated to 2.0×10^6 cells/ml density after overnight growth in SC-URA glucose at 30°C. At 0, 6, 12, 18, 24, 36, and 48 hours, duplicate measurements were taken from each sample. One ml of cell culture was pipetted into a cuvet to measure absorbance at 600 nm using a Hitachi U-2000 Spectrophotometer. Spectroscopic growth analysis was performed at least three times for each yeast strain.

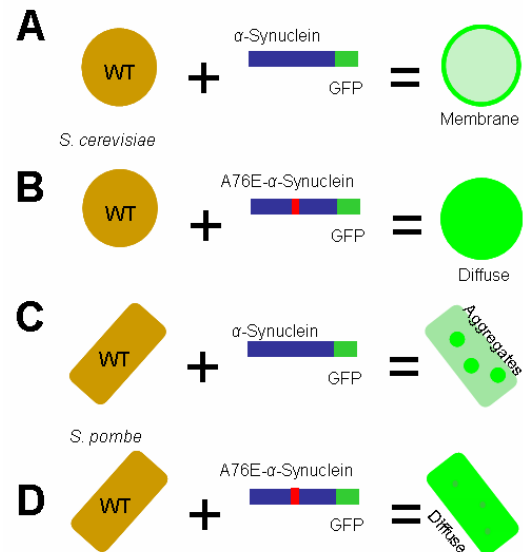


Figure 5. Hypothesis for A76E- α -Synuclein Localization in Budding and Fission Yeast. A. WT- α -Synuclein-GFP in *S. cerevisiae*. WT- α -synuclein localizes to the plasma membrane in budding yeast at 24 hours of induction. B. A76E- α -Synuclein-GFP in *S. pombe*. I hypothesized that A76E- α -synuclein will delay membrane localization and remain cytoplasmically diffuse at 24 hours of induction. C. WT- α -Synuclein-GFP in *S. pombe*. Expression of WT- α -synuclein in fission yeast produces aggregates at 24 hours of expression. D. A76E- α -Synuclein-GFP in *S. pombe*. I hypothesized that A76E- α -synuclein expression in fission yeast will delay aggregation at 24 hours of induction.

Construct	Expression Vector	Strain
WT- α -Synuclein-GFP	pYES2.1	<i>kgd1</i> Δ <i>glo4</i> Δ
A30P- α -Synuclein-GFP	pYES2.1	<i>kgd1</i> Δ <i>glo4</i> Δ
A53T- α -Synuclein-GFP	pYES2.1	<i>kgd1</i> Δ <i>glo4</i> Δ
E46K- α -Synuclein-GFP	pYES2.1	<i>kgd1</i> Δ <i>glo4</i> Δ
GFP	pYES2.1	<i>kgd1</i> Δ <i>glo4</i> Δ
No cDNA (Parent Plasmid)	pYES2.1	<i>kgd1</i> Δ <i>glo4</i> Δ
WT- α -Synuclein (no GFP)	pYES2.1	<i>kgd1</i> Δ

Table 1. List of Transformed Budding Yeast Strains for Chapter 1

Spotting Growth Analysis.

Cells were grown for 12 hours in SC-URA glucose at 30°C and adjusted to equal concentrations (2×10^7 cells/ml), serially diluted (five-fold) into 96-well microwell plates and spotted on SC-URA glucose (2%) and galactose (2%) plates using a 48-prong frogger (Dan-Kar). For each spotting, three trials were carried out using the same microwell plate. This analysis was repeated at least twice for each yeast strain.

Fluorescence Microscopy.

Cells were visualized under a Nikon TE2000-U fluorescent microscope and images were acquired using the Metamorph 4.0 imaging software. About 750 to 1000 cells were counted at several time-intervals depicted in the growth-rate analysis (18, 24, 36, and 48 hours). For a qualitative analysis, three qualities were assessed and scored: plasma-membrane localization, cytoplasmic aggregates, and/or diffuse fluorescence. A ratio of the fluorescence patterns was created by characterizing about 750 cells according to their dominant phenotype: aggregate, diffuse, or membrane. Non-fluorescent cells were included in the total count to account for general expression levels.

Results

*α -Synuclein Progressively Loses Membrane Localization and Forms Aggregates in *kgd1* Δ*

We evaluated the localization of α -synuclein in *kgd1* Δ against the BY4741 parent strain to understand its properties under conditions of mitochondrial dysfunction. At four time points, 18, 24, 36, and 48 hours, fluorescence images were captured to assess the localization of α -synuclein-GFP. At 18 and 24 hours of induction, *kgd1* Δ and BY4741 yeast were phenotypically identical (phenotype not shown for 18 hours; Figure 6 and 7). Yeast containing the parent pYES2.1 vector did not fluoresce (not shown). Cells with the GFP plasmid showed diffuse fluorescence in the cytoplasm, but not the vacuole. WT- α -synuclein expression showed intense plasma membrane localization with little or no diffuse fluorescence. A30P,

A53T, and E46K exhibited a combination of cytoplasmically diffuse, aggregate, and plasma membrane localized fluorescence patterns.

At 36 hours of expression, the *kgd1* Δ fluorescence phenotype slightly differed from its parent BY4741. A fraction of GFP-expressing cells showed aggregation by forming distinct foci (i.e. concentrated pixel intensity). The α -synuclein isoforms exhibited similar findings. Then, at 48 hours (Figure 6 and 7), this change was more prominent. In all *kgd1* Δ α -synuclein-expressing cells, aggregates of α -synuclein were observed in higher numbers than BY4741 cells. Strikingly, WT, A53T, and E46K lost plasma membrane localization, whereupon cytoplasmic inclusions were found. These inclusions were in close proximity to the plasma membrane and seemingly attached at 48 hours. This result is noted by decreased plasma membrane fluorescence and increased inclusion presence near the cell wall. Surprisingly, inclusions found at 24 hours of expression were not near the plasma membrane, but were situated near the vacuole, however, not inside the vacuole (Figure 7A).

The images captured over 48 hours were then quantified according to only three attributes: cytoplasmically diffuse, plasma membrane localized, and formation of foci or aggregates. In *kgd1* Δ , GFP and all isoforms of α -synuclein showed a gradual progression to aggregate formation in a time-dependent manner. Aggregate formation was accompanied by loss of localization in each characteristic area. Thus, A30P-expressing *kgd1* Δ cells lost both membrane and cytoplasmic localization as aggregates formed.

Approximately one out of seventy-five cells in both *kgd1* Δ and BY4741 exhibited complete auto-fluorescence in each yeast strain. As the cells aged, this phenotype became more prevalent. Under DIC microscopy, these cells were smaller and displayed an irregular margin. Closer inspection revealed no vesicular trafficking or cytoplasmic activity, which is suggestive of cell death. Further analysis will have to be carried out to determine their exact fate. These cells were counted as diffuse. For example, in BY4741 WT- α -synuclein-expressing cells, the quantified ratio shows some diffuse cells.

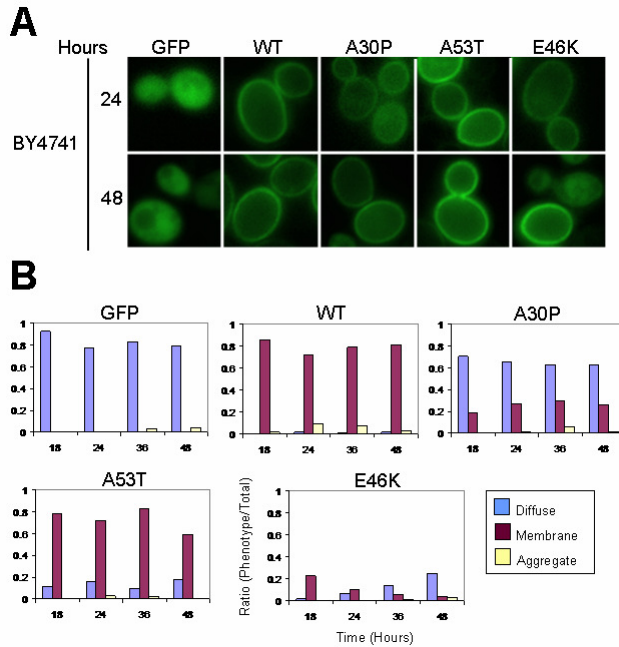


Figure 6. α -Synuclein Localization in the Strain BY4741. A. *Fluorescence Images.* Images captured of *S. cerevisiae* BY4741 at 24 and 48 hours of α -synuclein expression are shown. BY4741 cells show plasma membrane localization of α -synuclein-expressing cells at 24 and 48 hours of induction as described in Sharma et. al. (2006). B. *Quantification.* The ratio of the three fluorescence patterns (i.e. diffuse, membrane, aggregate) was scored from 750 cells at 18, 24, 36, and 48 hours. WT, A53T, and E46K α -synuclein show plasma membrane localization. Both GFP and A30P predominantly show cytoplasmic localization. Minimal aggregates were observed under each condition. E46K, in general, displays less fluorescence.

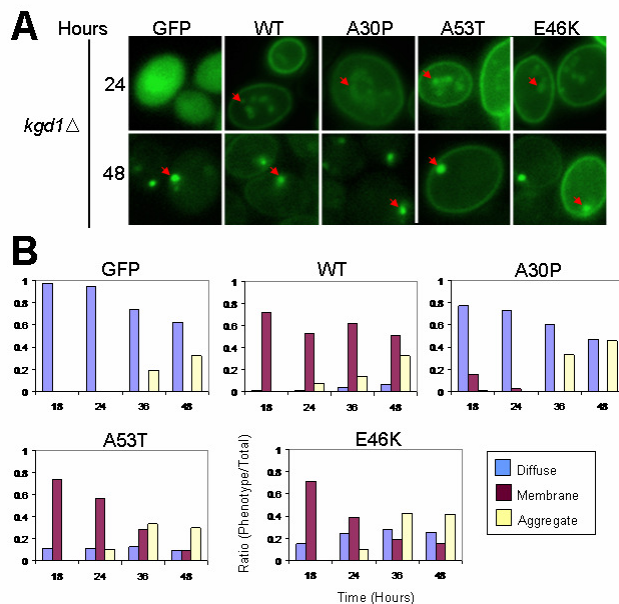


Figure 7. α -Synuclein Localization in the Strain *kgd1* Δ . A. *Fluorescence Images.* Images captured of *S. cerevisiae* *kgd1* Δ at 24 and 48 hours of α -synuclein expression are shown. In all samples, aggregates generally begin to appear at 24 hours, located in the cytoplasm. At 48 hours, aggregates form near the membrane (red arrows). B. *Quantification.* The ratio of the three fluorescence patterns (i.e. diffuse, membrane, aggregate) was scored from 750 cells at 18, 24, 36, and 48 hours. GFP-expressing cells begin to exhibit aggregates at 36 hours which is enhanced at 48 hours. Cytoplasmic localization steadily decreases over 48 hours. A30P- α -synuclein-expressing cells display a diffuse phenotype, which decreases in number as aggregates begin to form at 36 hours. WT, A53T, and E46K α -synuclein-expressing cells all show membrane localization at 18 hours which also steadily declines as aggregates form at 24 hours.

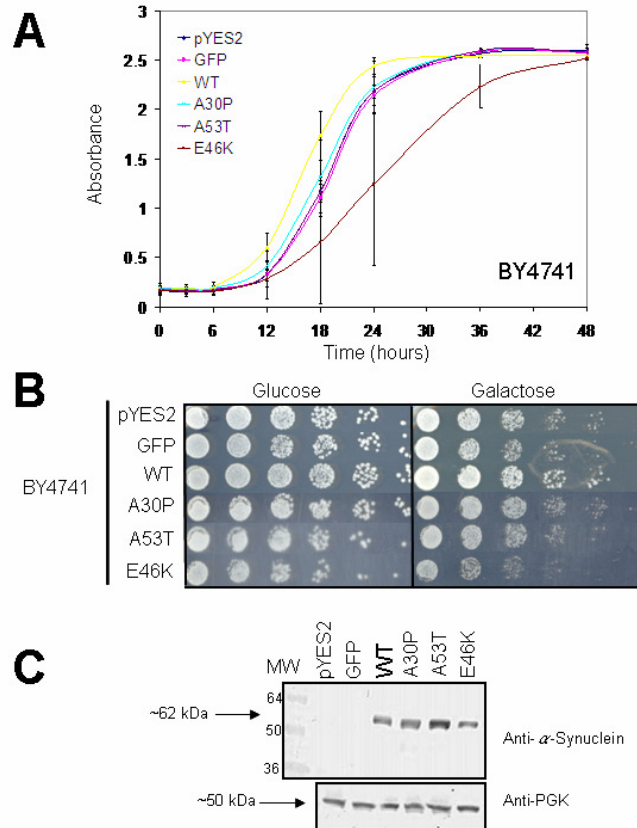


Figure 8. Growth Analysis and Expression of α -Synuclein in the Strain BY4741. A. *Growth Curve.* OD600 was assessed over a 48-hour time course where toxicity was observed only in E46K- α -synuclein cells. Error bars represent standard deviation from three separate growth analyses. B. *Serial Spotting.* Growth was also assessed by serially diluting yeast cells fivefold in non-inducing (glucose) and inducing (galactose) media. E46K-expressing cells also displayed diminished growth under spotting. Both the growth curve and spotting analyses show that GFP has no effect on budding yeast growth.

*α -Synuclein is not Toxic in *kgd1* Δ*

Next we examined toxicity of *kgd1* Δ by using a spectroscopic (OD_{600nm}) growth-rate analysis. This technique utilizes the density of cells to correlate degree of toxicity in actively dividing yeast. Error bars represent the standard deviation from three different trials. In the BY4741 parent strain, with the *kgd1* gene, toxicity was observed with the E46K- α -synuclein isoform (Figure 8A).

This result was also confirmed with the serial spotting growth analysis, where diminished growth was observed on inducing media (galactose) in E46K- α -synuclein-expressing cells (Figure 8B). Glucose served as a loading control to ensure equal cell concentrations in each plasmid condition. Since equal growth was observed on the glucose media, this control allowed us to directly compare growth on galactose plates, which turn-on protein expression.

However, in the *kgd1* Δ strain, no toxicity was observed in either growth analysis (Figure 9A and 9B). Interestingly, *kgd1* Δ cells had a faster doubling-time when compared to BY4741 at 12-hours of growth in log phase (Figure 8A and 9A).

*α -Synuclein Expression is Decreased in *kgd1* Δ*

To address the lack of toxicity, α -Synuclein expression was measured in *kgd1* Δ . At 24 hours of induction, all *kgd1* Δ strains showed significantly reduced expression

when compared to BY4741 strains (Figure 9C). Interestingly, the fluorescence phenotype between both yeast strains showed roughly equivalent α -synuclein expression. Thus, the fluorescence phenotype cannot be used as an indicator of α -synuclein concentration.

These results prompted induction of both strains for a 72-hour time-course to evaluate the change of α -synuclein expression over a longer period of time. I hypothesized that α -synuclein concentration would increase by 72-hours. Thus, lysates were prepared at three time points: 24, 48, and 72 hours for GFP and WT-GFP in *kgd1* Δ , where BY4741 WT-GFP served as a control. Surprisingly, protein concentration in neither GFP nor WT-GFP expressing *kgd1* Δ cells changed (Figure 10A).

Since GFP tagged WT- α -synuclein was used in figure 10A, I wanted to determine whether low expression was an α -synuclein specific effect or due to GFP. Thus, WT- α -synuclein (no GFP) was transformed into *kgd1* Δ to evaluate expression without GFP. Surprisingly, WT- α -synuclein (no GFP) in *kgd1* Δ displayed low expression when compared to BY4741 at 24 hours of induction (Figure 10B). Additionally, LacZ, a harmless reporter gene, was also transformed into *kgd1* Δ to evaluate expression of "any" protein, in general. LacZ also showed diminished expression (data not shown). These data suggest that most foreign protein transformed into *kgd1* Δ would reveal decreased

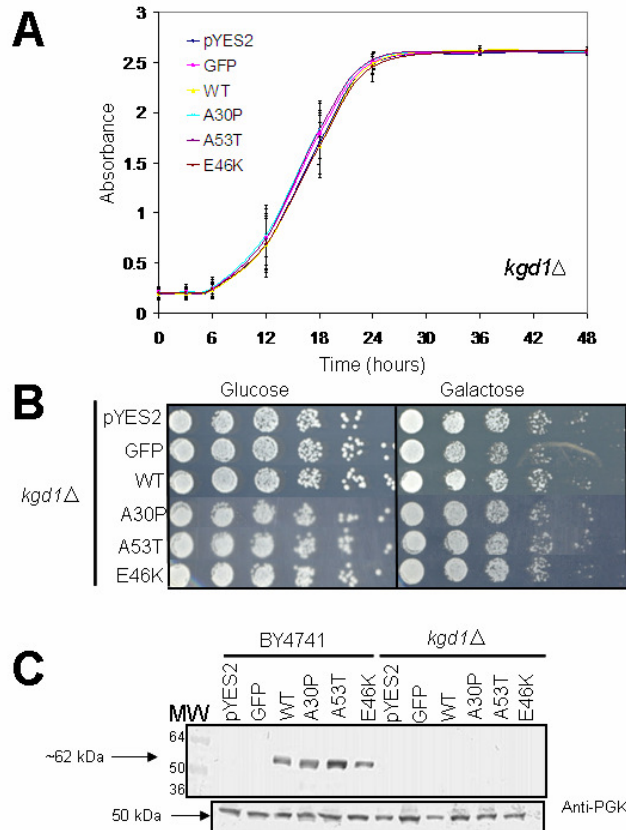


Figure 9. Growth Analysis and Expression of α -Synuclein in the Strain *kgd1Δ*. A. *Growth Curve.* OD600 was assessed over a 48-hour time course with no observed toxicity. Error bars represent standard deviation from three separate growth analyses. B. *Serial Spotting.* Growth was also assessed by serially diluting yeast cells fivefold in non-inducing (glucose) and inducing (galactose) media. No toxicity observed. Both the growth curve and spotting analyses show that GFP has no effect on *kgd1Δ* budding yeast growth. C. *Western Blot.* For all samples, expression was induced for 24 hours and detected using an anti- α -synuclein monoclonal primary antibody (1:2000). The isogenic parent strain, BY4741, was used as a control to compare expression between BY4741 and *kgd1Δ*. In *kgd1Δ*, however, all α -synuclein-expressing cells displayed decreased expression. Anti-phosphoglycerate kinase (PGK) primary monoclonal antibody (1:5000) was used as a loading control.

expression compared to its isogenic parent strain, BY4741.

In figure 10B, when we compare expression of each condition between BY4741 and *kgd1Δ*, we see that *kgd1Δ* has overall decreased expression. However, this does not tell us whether GFP or α -synuclein alone is having an effect on expression. To determine this, we must look at expression within each strain and not between strains. WT- α -synuclein (no GFP) expressed in BY4741 and *kgd1Δ* shows enhanced expression when compared to WT- α -synuclein-GFP in both strains, respectively. Thus, GFP is causing decreased expression in both strains.

*α -Synuclein Localization in *glo4Δ* does not Change*

In another mitochondrial mutant, *glo4Δ*, α -synuclein localization was remarkably similar to BY4741 (Figure 5 and 11). The quantification of the *glo4Δ* phenotype reveals fluorescence patterns that are nearly identical to the isogenic parent strain, BY4741. The only difference is that E46K- α -synuclein expressing *glo4Δ* cells have a higher number of cells that fluoresce when compared to BY4741 cells. Again, the number of cells that fluoresce is not indicative of protein expression.

*α -Synuclein is not Toxic in *glo4Δ**

We next evaluated whether or not α -synuclein was toxic to the strain *glo4Δ*. No toxicity was observed in *glo4Δ* from either spectroscopic growth-rate analysis (Figure 12A) or serial spotting (Figure 12B). Some variation was observed in the first 12 hours of growth, which is within the standard deviation of three trials. Compared to *kgd1Δ*, the doubling-time of *glo4Δ* is not as fast. Since α -synuclein was not found to be toxic in *glo4Δ* or *kgd1Δ*, plus *kgd1Δ* exhibited low expression, we expected to observe diminished expression in *glo4Δ*, as well.

*α -Synuclein Expression in *glo4Δ* is Lower than BY4741, but not *kgd1Δ**

We measured the expression of α -synuclein to determine if low expression was correlated with low toxicity. At 24 hours of induction, BY4741 was again noted to have decreased E46K- α -synuclein expression (Figure 12C). All isoforms of α -synuclein and GFP displayed decreased expression in *glo4Δ* when compared to BY4741, but not nearly as severe as *kgd1Δ*. No further expression analysis was completed as done in *kgd1Δ*.

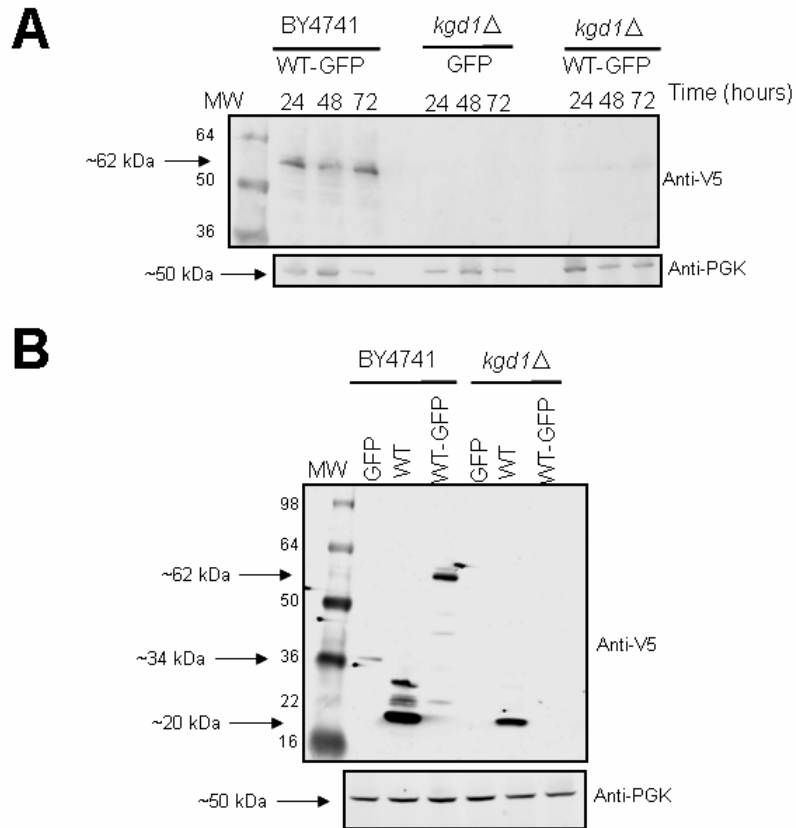


Figure 10. Time-Course and Non-GFP Tagged WT- α -Synuclein Expression in BY4741 and *kgd1*Δ Yeast Strains. A. 72-Hour Time Course Western Blot. In GFP and WT- α -Synuclein-expressing *kgd1*Δ cells, expression did not change over a 72-hour period. B. Effect of GFP on *kgd1*Δ. Compared to BY4741, all foreign proteins in *kgd1*Δ had diminished expression. Additionally, non-GFP tagged WT- α -Synuclein in BY4741 exhibited increased expression and variable banding when compared to WT- α -Synuclein-GFP. Anti-phosphoglycerate kinase (PGK) primary monoclonal antibody (1:5000) was used as a loading control in both experiments.

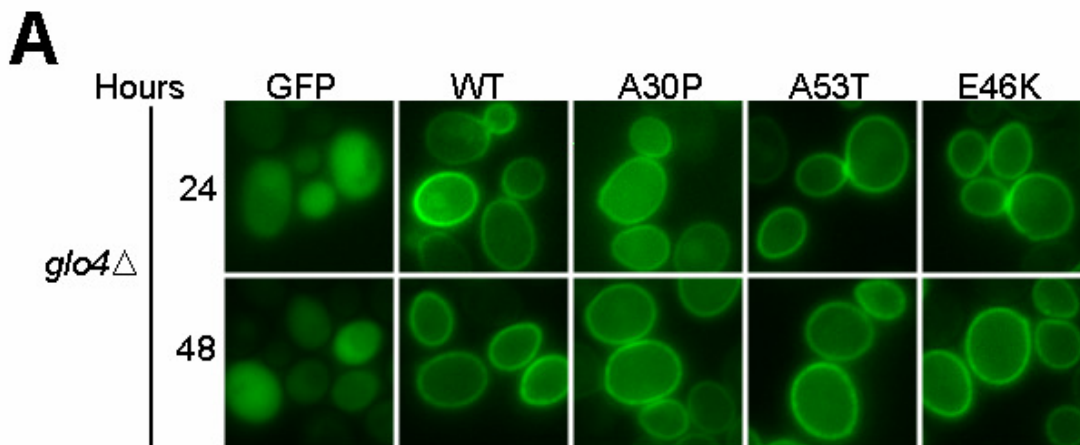
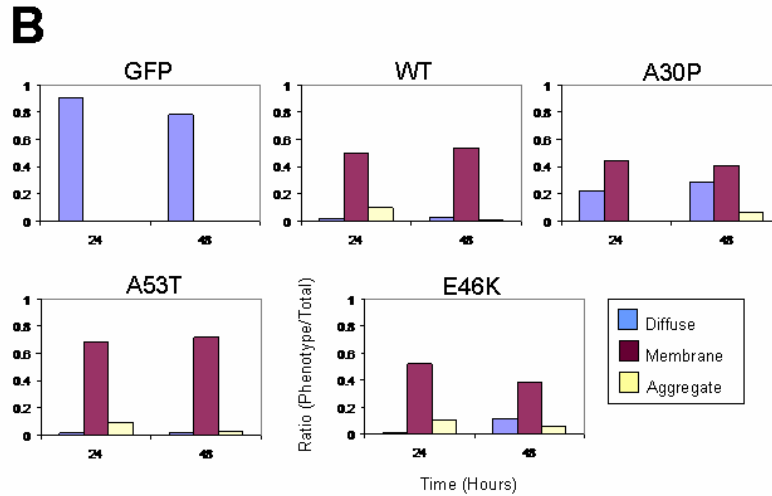


Figure 11. α -Synuclein Localization in the Strain *glo4*Δ. A. Fluorescence Images. Images captured of *S. cerevisiae glo4*Δ at 24 and 48 hours of α -synuclein expression are shown. *glo4*Δ cells show plasma membrane localization of α -synuclein-expressing cells at 24 and 48 hours of induction.



B. Quantification. The ratio of the three fluorescence patterns (i.e. diffuse, membrane, aggregate) was scored from 750 cells at 24 and 48 hours. WT, A53T, and E46K α -synuclein show plasma membrane localization. A30P- α -synuclein displays a mix of plasma membrane and cytoplasmic localization. GFP predominantly shows cytoplasmic localization. Minimal aggregates were observed under each condition.

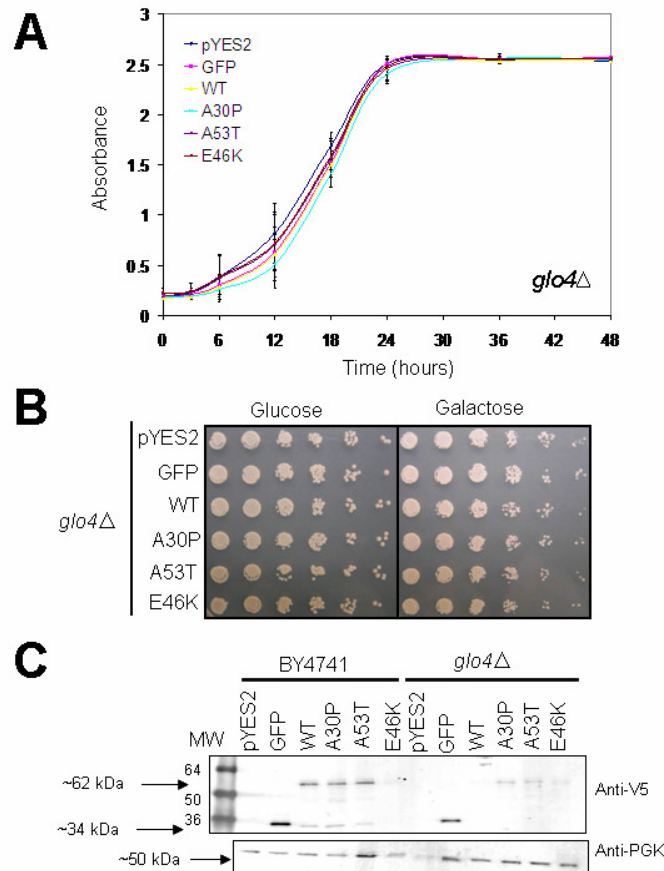


Figure 12. Growth Analysis and Expression of α -Synuclein in the Strain *glo4* Δ . **A. Growth Curve.** OD600 was assessed over a 48-hour time course with no observed toxicity. Error bars represent standard deviation from three separate growth analyses. **B. Serial Spotting.** Growth was also assessed by serially diluting yeast cells fivefold in non-inducing (glucose) and inducing (galactose) media. No toxicity observed. Both the growth curve and spotting analyses show that GFP has no affect on *glo4* Δ budding yeast growth. **C. Western Blot.** For all samples, expression was induced for 24 hours and detected using an anti-V5 monoclonal primary antibody (1:5000). The isogenic parent strain, BY4741, was used as a control to compare expression between BY4741 and *glo4* Δ . In BY4741, decreased E46K- α -synuclein expression was observed again. In *glo4* Δ , however, all α -synuclein-expressing cells displayed decreased expression. GFP expression was also in decreased in *glo4* Δ comparison to BY4741. Anti-phosphoglycerate kinase (PGK) primary monoclonal antibody (1:5000) was used as a loading control.

Thus, lowered expression was found to be correlated with low toxicity. Seemingly, lower expression in *kgd1Δ* compared to *glo4Δ*, allowed *kgd1Δ* to grow slightly faster despite the presence of aggregates.

Discussion

The complex interplay between oxidative stress and α -synuclein folding is becoming clearer as we evaluate the role of the mitochondria in Parkinson's disease. Here, I evaluated two yeast strains with different mitochondrial mutations, *kgd1Δ* and *glo4Δ*. Both gene deletions affected α -synuclein aggregation and toxicity in different manners.

Toxicity was not observed in both knockout strains even after the addition of α -synuclein. Both knockout strains exhibited decreased expression when compared to their isogenic parent strain, BY4741. Finally, only *kgd1Δ* displayed time-dependent aggregate formation in all GFP-related proteins combined with the least expression observed.

Does Decreased α -Synuclein Expression Diminish Toxicity?

One common theme of no toxicity in *kgd1Δ* and *glo4Δ* cells is the lack of moderate α -synuclein to challenge the cells. Lowered expression may be a protective mechanism for the cell. Since toxicity was not observed in these two cases, we can suggest that toxicity is related to levels of α -synuclein.

Interestingly, toxicity was observed in low-expressing E46K- α -synuclein BY4741 cells (Figure 7). This is contradictory to the result seen in both *kgd1Δ* and *glo4Δ* cells (Figure 9 and 12). Here we could suggest that E46K is more toxic than all other α -synuclein isoforms. Yet, why don't we see toxicity in E46K-expressing *kgd1Δ* and *glo4Δ* cells?

Despite low α -synuclein expression, only *kgd1Δ* displays the formation of aggregates. Aggregates may be protective in *kgd1Δ* cells, thus E46K would be inactive to cause harm to the cell. This may be due to ROS generation by inhibition of mitochondrial complex I (Figure 4). Enhanced ROS content may induce general protein misfolding in the cell by disrupting cellular machinery necessary for proper protein folding.

However, *glo4Δ* does not have aggregates or toxicity. It is important to note that aggregates are not a requirement for toxicity. Also, lack of aggregates does not imply toxicity (Conway *et al.*, 1998). What compensatory mechanism does *glo4Δ* have to reduce E46K-based toxicity? The *glo4Δ* strain lacks a pivotal antioxidant, but does not generate ROS as a result. Since ROS formation is not induced in *glo4Δ*, maybe the cell overcompensated for the lack of antioxidants by expressing other proteins to clear excess ROS. Thus, the cell may have not been in a toxic state from the very beginning. Also, since we did not challenge the cells with any oxidants, we do not know the threshold at which protein aggregation would commence within *glo4Δ* cells.

Additionally, in previous studies within our lab, no aggregates were observed in compromised cells lacking manganese superoxide dismutase but with α -synuclein and hydrogen peroxide (Sharma *et al.*, 2006). Thus, toxicity was observed without visible protein aggregation. More research must be done to uncover the toxic element within these cells.

Are Aggregates Protective?

Intense debate in the field of neurodegenerative diseases strives to understand if aggregates are toxic or protective. Since α -synuclein-rich Lewy bodies are correlated with Parkinson's disease, much investigation has gone into understanding why and how α -synuclein aggregates (Spillantini *et al.*, 1998). In *kgd1Δ*, toxicity is absent but aggregates are not. Thus, the combination with low expression and aggregation may be a protective mechanism for the cell. Additionally, since aggregates do not form until 36 to 48 hours of expression, we cannot determine whether or not they are toxic since growth reached a plateau phase at that time.

Emerging evidence suggests that circular trimeric protofibrils are the toxic agent in NDD (Lashuel *et al.*, 2002). Through a pore-like mechanism they can permeabilize a membrane or vesicle which diminishes the integrity of the cell. Protofibrils are the intermediate of fibrils and are thought to contribute to cytotoxicity more than larger aggregates. In our investigation, toxicity is observed only in the E46K-expressing BY4741 cells. Since aggregates are not readily found under this condition, we can suggest that this model supports the protofibril hypothesis due to membrane localization in fluorescent cells. Also, within our fission yeast model (Chapter 2), toxicity is also absent in cells with abundant aggregates.

Where do α -Synuclein Aggregates Localize?

It is important to note that aggregation observed in *kgd1Δ* begins within the cells' interior at 24 hours and moves to the membrane at 48 hours. We are not sure whether or not the membrane aggregates observed at 48 hours are formed from loss of membrane localization or vesicular transport to the membrane (Caughey *et al.*, 2003). One clue points to vesicular transport. Since GFP also forms these characteristic aggregates, plasma membrane localization is not necessary for membrane-bound aggregate formation. The same argument applies for A30P- α -synuclein. Yet, this does not discount the idea that retrograde vesicular transport from the membrane may create these distinct aggregates. Both pathways may be operating.

Does Genetic Diversity in the Mitochondria Change α -Synuclein's Properties?

Our laboratory's investigation of three mitochondrial mutants have regulated α -synuclein's aggregation and toxicity in three completely different ways. In summary, *kgd1Δ* cells showed aggregation with no toxicity; *glo4Δ* cells displayed no aggregation with no toxicity; and *sod2Δ* cells (lacking manganese superoxide dismutase) exhibited toxicity without aggregation. This research immediately points to the complexity of mitochondrial dysfunction in Parkinson's disease. Slight differences within any of these genes will regulate α -synuclein properties in very different ways. Thus, aging and the accumulation of oxidants will also be different. Yet, one conclusion can be made: α -synuclein interacts with the mitochondria in PD pathogenesis.

Construct	Expression Vector	Strain
A76E- α -Synuclein-GFP	pYES2.1	BY4741
A76E- α -Synuclein-GFP	pNMT1	TCP1

Table 2. List of Transformed Budding and Fission Yeast Strains for Chapter 2

Chapter 2: The A76E α -Synuclein Mutation Reduces Aggregation in Fission Yeast

Materials and Methods

Please refer to *Chapter 1: Mitochondrial Mutants for complete experimental procedures in S. cerevisiae*. Methods adapted from Brandis et. al. (2006).

S. cerevisiae expression vectors.

A76E mutant α -synuclein was created from WT- α -synuclein using GeneTailor™ Site-Directed Mutagenesis in a pYES2.1/TOPO expression vector (Table 2 and Figure 13 and 14; Invitrogen).

S. pombe expression vectors.

A76E mutant α -synuclein was created from WT- α -synuclein using GeneTailor™ Site-Directed Mutagenesis in a pNMT-1 TOPO-TA expression vector (Table 2 and Figure 13 and 14; Invitrogen).

Yeast Strains.

BY4741 (*MATa his3 Δ 1 leu2 Δ 0 met15 Δ 0 ura3 Δ 0*) was purchased from Open Biosystems (Huntsville, AL). TCP1 (*h- leu1-32*; Invitrogen)

Yeast Transformation.

S. cerevisiae and *S. pombe* strains were transformed with the pYES2.1 and pNMT-1 vectors, respectively, using the lithium-acetate transformation method (Alfa et. al., 1993).

Fluorescence Microscopy.

S. pombe cells were grown overnight at 30 °C in Edinburgh Minimal Medium (EMM; Invitrogen) containing thiamine (10 μ M; to repress α -synuclein expression). After 24 hours, cells were pelleted at 1500xg for 5 min, washed twice in 10 mL dH₂O, resuspended in 10 mL EMM without thiamine, of which 125 μ l of cells were used to inoculate 25 mL EMM without thiamine (to express α -synuclein). Cells were viewed using a Nikon TE-2000U fluorescence microscope at 1000X magnification. Images were deconvoluted using the MetaMorph version 4.2 software. To quantify α -synuclein aggregates in Figure 13, cells were first viewed under differential interference contrast (DIC) microscopy and total cell count in the field was determined. The same cells in the field were then viewed for GFP fluorescence. The number of cells in the field containing 1, 2, or 3+ aggregates or a diffuse phenotype was determined. At least 750 cells were evaluated for each condition. Aggregates were scored as ratio of total cells in the field that expressed 1, 2, and 3+ aggregates, or a diffuse phenotype.

Protein Expression.

Lysates of *S. pombe* expressing α -synuclein, protein electrophoresis, and Western blotting, were performed as reported for *S. cerevisiae* in Sharma, 2004. The monoclonal anti-V5 antibody-AP (Invitrogen; 1:5000 dilution) was used for protein detection. Anti- β -actin

primary monoclonal antibody (1:2500) was used as a loading control for *S. pombe* only.

Growth Curve.

Transformed cells were grown in 10 mL EMM + thiamine overnight at 30 °C, 200 rpm. Cells were harvested at 1500 x g for 5 min at 4°C, washed twice in 5 mL dH₂O, re-suspended in 5 mL dH₂O and counted. Flasks with 25 mL EMM + thiamine or EMM – thiamine, were each inoculated to 2.0x10⁶ cells/mL density. At 0, 3, 6, 12, 18, 24, and 36 hours, OD600 absorbance of one mL cell culture (in duplicate) was measured using a Hitachi U-2000 Spectrophotometer. Averaged absorbance readings were plotted against time points.

Serial Spotting.

For spotting, transformed cells were grown to mid-log phase in EMM + thiamine, normalized to equal densities (2x10⁷ cells/ml), serially diluted (five-fold) into 96-well microtiter plates and spotted on EMM + thiamine or EMM - thiamine plates using a 48-prong frogger (Dan-Kar) or manual pipeting. Images were photographed after two days of growth.

Results

A76E- α -Synuclein Localizes to the Membrane More Slowly

We first asked if the A76E- α -synuclein mutation would change membrane binding affinity in budding yeast. At 24 hours of expression, A76E- α -synuclein displayed a diffuse phenotype mixed with plasma membrane localization in BY4741 (Figure 15A and 15B), similar to A30P- α -synuclein (Figure 6). At 48 hours, plasma membrane localization became the dominant phenotype with little to no cytoplasmic localization. At the same time point, A30P- α -synuclein remains in the cytosol (Figure 6). Thus, the A76E- α -synuclein mutation is distinctly different from A30P- α -synuclein. WT- α -synuclein did not produce a diffuse phenotype as observed in A76E- α -synuclein-expressing cells at 24 hours. Yet, at 48 hours, A76E- α -synuclein resembled the WT- α -synuclein phenotype.

A76E- α -Synuclein Reduces the Rate of Aggregation

Next, we examined if A76E- α -synuclein reduces its rate of aggregation. In fission yeast, a similar phenomenon occurred. A mixed diffuse and aggregate phenotype was observed in A76E- α -synuclein-expressing cells at 24 hours (Figure 15C and 15D). By 48 hours, however, A76E- α -synuclein translocated from the cytoplasm to the plasma membrane. Yet, the total number of fluorescing cells decreased at 48 hours (Figure 15 D). As expected, WT- α -synuclein did not produce a diffuse phenotype as observed in A76E- α -synuclein-expressing cells at 24 hours. At 48 hours, WT- α -synuclein appeared distinctly different from A76E- α -synuclein.

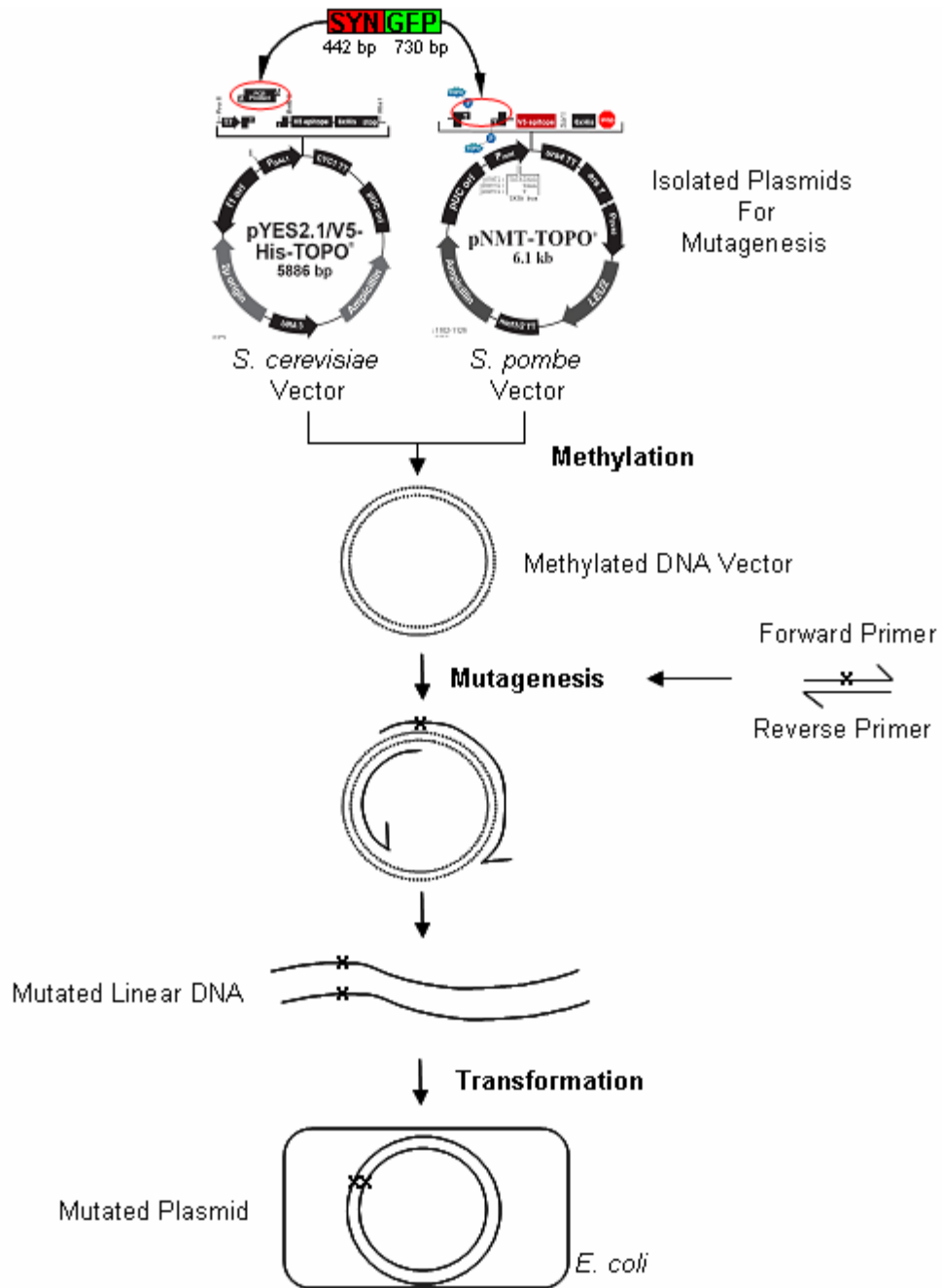


Figure 13. Diagrammatic Flowchart for Mutagenesis. Adapted from GeneTailor™ Site-Directed Mutagenesis (Invitrogen). For each expression vector, pNMT1 and pYES2, the A76E mutation was created in α -synuclein. Thus, each vector underwent a separate mutagenesis reaction. Each vector was first methylated with DNA methylase for 1 hour at 37 °C. The methylated DNA was then used for PCR amplification with two overlapping primers, one of which contained the desired mutation. This reaction yielded mutated DNA along with the methylated template DNA. The products were transformed into *E. coli* which circularized the linear DNA and digested the methylated template. The plasmid was isolated once again and sequenced at The University of Chicago (Chicago, IL).

A Normal α -Synuclein (76th Codon is Red):
 5'-GTTGGAGGAGGAGCAGTGGTGACGGGTGTGACAGCAGTAGCCCAGA-3'
 Mutant A76E- α -Synuclein (76th Codon is Red):
 5'-GTTGGAGGAGGAGCAGTGGTGACGGGTGTGACAGCAGTAGCCCAGA-3'
 Reverse Non-Mutagenesis Primer:
 3'-CAACCTCCTCGTCAACCTGCCCACACTGT-5' (T_m = 68.2 °C)
 Forward Mutagenesis Primer for Alanine (A) to Glutamic Acid (E) Mutation:
 5'-CAGTGGTGACGGGTGTGACAGAAAGTAGCCCAGA-3' (T_m = 68.1 °C)

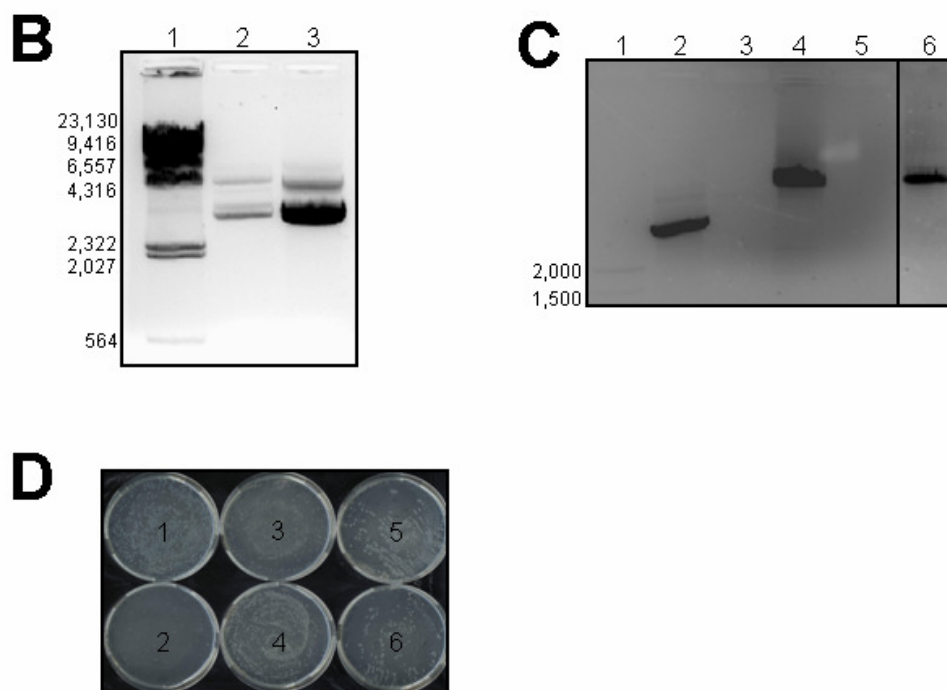


Figure 14. A76E- α -Synuclein-GFP Site-Directed Mutagenesis. The A76E- α -Synuclein-GFP mutation was created using the GeneTailor™ Site-Directed Mutagenesis System (Invitrogen). **A. Primer Design.** The forward mutagenesis primer was designed to change one nucleotide, within the 76th codon of α -synuclein-GFP (C-terminus), from Cytosine (C) to Adenine (A). The mutation of one nucleotide from C to A changes the 76th codon to glutamic acid (E) instead of alanine (A). Oligonucleotides were ordered from Operon (Qiagen). **B. Plasmid DNA Isolation.** DNA plasmid vectors, pYES2 (lane 2) and pNMT-1 (lane 3) containing WT- α -synuclein fused with GFP at the Carboxy-terminal domain, were isolated from *E. coli* stored at -80 °C using the QIAprep Spin Miniprep Kit (Qiagen). 1: λ /HIND III Ladder (base pairs), 2: pYES2 WT- α -Synuclein-GFP, 3: pNMT-1 WT- α -Synuclein-GFP. **C. Mutagenesis Reaction.** Polymerase Chain Reaction (PCR) reagents and primers containing the target mutation were combined with the a methylated target plasmid for the mutagenesis. Taq polymerase allows the reaction to proceed. Reactions lacking Taq served as negative controls. Mutagenesis products for the pNMT-1 and pYES2 vectors are seen in lane 4 and 6, respectively. 1: AmpliSize Ladder (base pairs), 2: Positive Control pYES2 Plasmid, 3: -Taq pNMT-1 WT- α -Syn-GFP, 4: +Taq pNMT-1 WT- α -Syn-GFP, 5: -Taq pYES2 WT- α -Syn-GFP, 6: +Taq pYES2 WT- α -Syn-GFP. **D. Transformed DH5 α -T1 *E. coli* with Mutated Vectors.** All plates were made with ampicillin (50 μ g/mL) and X-gal (100 μ g/mL) to select for non-transformed *E. coli* and screen blue/white colonies, respectively (i.e. white indicates a successful transformation and functional lacZ gene). Positive control, plate 1, was transformed with a pUC19 vector containing an ampicillin resistance gene, which was supplied by the mutagenesis kit (Qiagen). The negative control, plate 2, was not transformed with the pUC19, thus was not able to grow on the media. Plate 3 and 4 served as methylation controls where S-adenosylmethionine (SAM) enhances DNA methylation. Plate 3 shows that enhanced methylation increases the selectivity of colonies. Plate 5 and 6 are colonies of *E. coli* containing vectors with the human cDNA A76E- α -synuclein-GFP gene. Positive transformants were screened by bacterial whole cell PCR. Plasmid vectors were purified using a Qiagen mini-prep kit and the respective DNA sequences were confirmed at The University of Chicago Cancer Research Center DNA Sequencing Facility (Chicago, IL). 1: Positive Control, 2: Negative Control, 3: Methylation Control -SAM, 4: Methylation Control -SAM, 5: pNMT-1 A76E- α -Synuclein-GFP, 6: pYES2 A76E- α -Synuclein-GFP.

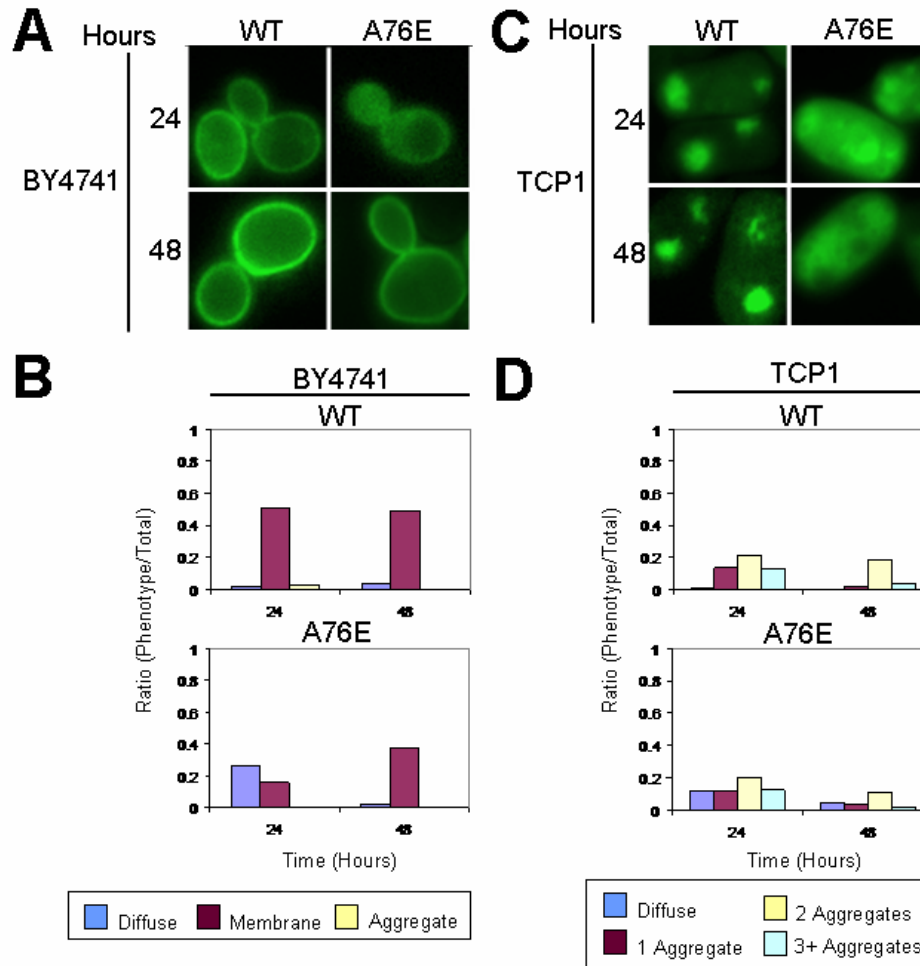


Figure 15. A76E- α -Synuclein Localization in BY4741 and TCP1 Yeast Strains. A & C. *Fluorescence Images.* Images captured of *S. cerevisiae* BY4741 and *S. pombe* TCP1 at 24 and 48 hours of α -synuclein expression are shown. B & D. *Quantification.* The ratio of different fluorescence patterns was scored from 750 cells at 24 and 48 hours. At 24 hours in BY4741, A76E- α -synuclein displayed cytoplasmic localization which moved to the membrane by 48 hours. At 24 hours in TCP1, A76E- α -synuclein exhibited a diffuse phenotype, also seen in A30P- α -synuclein-expressing *S. pombe* fission yeast (Brandis et. al., 2006). At 48 hours, this phenotype was less pronounced.

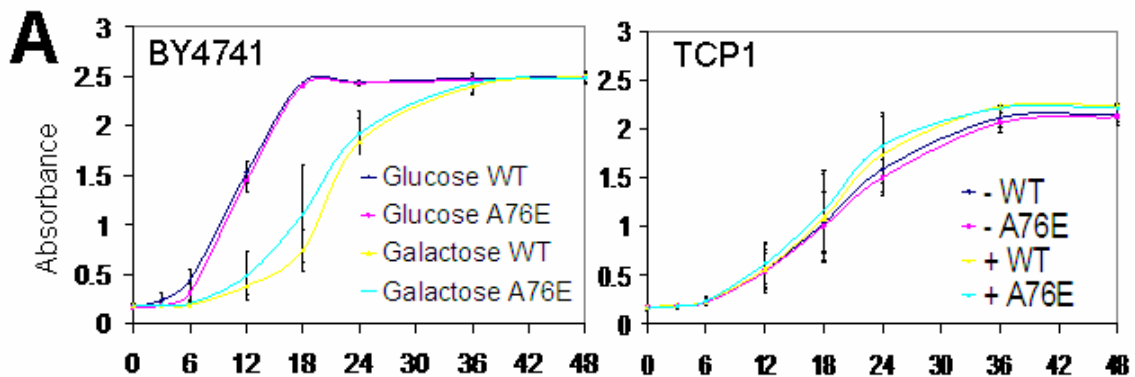
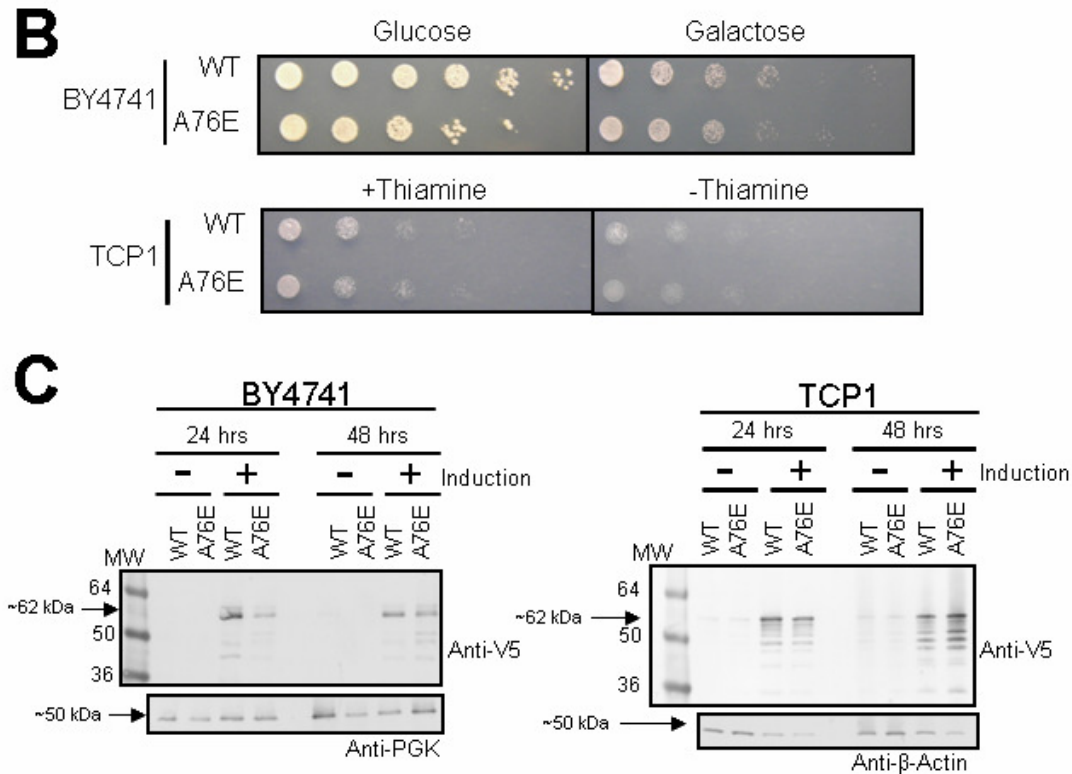


Figure 16. Growth Analysis and Expression of A76E- α -Synuclein in the Strains BY4741 and TCP1. A. *Growth Curve.* OD600 was assessed over a 48-hour time course with no observed toxicity in either BY4741 or TCP1. Both non-inducing (glucose and +thiamine) and inducing (galactose and -thiamine) growth conditions are shown with A76E- α -synuclein expression. Error bars represent standard deviation from three separate growth analyses.



B. Serial Spotting. Growth was also assessed by serially diluting yeast cells fivefold in non-inducing (glucose and +thiamine) and inducing (galactose and -thiamine) media. No toxicity observed. **C. Western Blot.** For all samples, expression was induced for 24 and 48 hours and detected using an anti-V5 monoclonal primary antibody (1:5000). In BY4741, A76E- α -synuclein expression is decreased only at 24 hours. In TCP1, WT and A76E α -synuclein expression is the same. Anti-phosphoglycerate kinase (PGK) primary monoclonal antibody (1:5000) was used as a loading control for budding yeast, *S. cerevisiae* BY4741. Anti- β -actin primary monoclonal antibody (1:2500) was used as a loading control for fission yeast, *S. pombe* TCP1.

No Toxicity Found in A76E- α -Synuclein-Expressing Yeasts

We next evaluated the growth of fission and budding yeast combined with A76E- α -synuclein. Growth analysis was done by expressing α -synuclein with EMM -Thiamine (pNMT vector is thiamine repressible). Thus, EMM +Thiamine represses the promoter and prevents expression, thereby serving as a loading control. Similarly, induction refers to the onset of protein expression. Thus, the induction of α -synuclein is not toxic to budding and fission yeast (Figure 16A and 16B).

Discussion

Our studies with A76E- α -synuclein have shown that a single amino acid substitution can change the aggregation kinetics of a pathogenic protein. Instead of creating A76E- α -synuclein and testing its properties *in vitro*, we utilized an *in vivo* approach in yeast to mimic the cellular stresses experienced by aging neurons.

In fission yeast, a full aggregation phenotype without diffuse fluorescence was delayed to 48 hours of expression (Figure 15). Thus, the mutation changed the shape of α -synuclein enough to prevent self-assembly for about 24 hours when compared to WT- α -synuclein (Figure 15A and 15B). In budding yeast, A76E- α -synuclein delayed full membrane localization for a similar 24 hour period.

How does the A76E Mutation Alter α -Synuclein Localization?

As described by Chiti and colleagues (2003), hydrophobicity, propensity of secondary structure conversion from α -helix to β -sheet, and charge allow us to mathematically characterize the aggregation rates of proteins and peptides. The A76E- α -synuclein mutation converted the 76th amino acid codon from methyl to glutamic acid which gave it an overall positive charge (Figure 17). The energy needed for it to form a β -sheet, pathogenic shape found in prions (Caughey *et. al.*, 2003), increased by a magnitude of ~ 1.5 . Thus, the dominant secondary shape would be α -helical. Finally, the mutation induced a threefold decrease in hydrophobicity. All of these factors combined account for a protein engineered for cytoplasmic solubility.

Is Decreased α -Synuclein Expression a Protective Mechanism?

Less expression in budding yeast at 24 hours coupled with cytoplasmic localization may be due to time and concentration-dependent assembly of proteins. Because at 48 hours of induction, A76E- α -synuclein begins to localize to the membrane from the cytoplasm and expression is also enhanced. Thus, over time, expression increases and so does assembly of α -synuclein to the membrane.

Additionally, toxicity was not observed at this time point. Decreased expression and lack of toxicity is

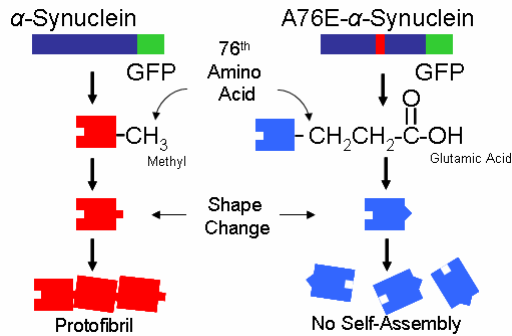


Figure 17. How Does A76E- α -Synuclein Delay Aggregation in Fission Yeast? Mutation Induces a Shape Change. The A76E mutation in α -synuclein must bring on a shape change, thereby postponing self-assembly. At a low pH, glutamic acid is negatively charged, which may aid in aggregate repulsion. Increased hydrophilicity, α -helix to β -sheet conversion, may also play a role as described in Chiti et. al. (2003).

consistent with out budding yeast knock-out models (Chapter 1).

What is the Toxic Species?

Lack of toxicity in the diffuse and aggregate states places a dichotomy between the protofibril and aggregate theory for toxicity. Since both phenotypes exist without toxicity, α -synuclein could be harmless to fission yeast. The phenotypes investigated here are similar to those found A30P- α -synuclein. Yet, A30P- α -synuclein does not aggregate in fission yeast to the degree of A76E- α -synuclein. However, investigations by Willingham et. al. (2003) have revealed 86 genes that protect against α -synuclein toxicity in budding yeast. A similar screen in fission yeast may reveal relevant genes that rescue PD pathogenesis (Brandis 2006). Thus, budding yeast may be adept to handling a toxic load of proteins due to its own genetic makeup.

Importantly, fission and budding yeast are separated by about 400 million years from their earliest evolutionary ancestor (Sipiczki et. al., 2000). The different phylogenies of both yeasts would undoubtedly contribute to a different genome and, thus, different handling of foreign proteins. As of now, we have not been able to induce toxicity within α -synuclein-expressing fission yeast. We believe that α -synuclein would be toxic when combined with an oxidizing substrate, such as hydrogen peroxide. The threshold for toxicity may then be reached.

A second possibility is a non-toxic protofibril model. There is no current scientific support for this theory, but it is a hypothesis that has not been refuted. Since there is lack of toxicity in both aggregate and cytoplasmic phenotypes in fission yeast, α -synuclein could be protective in both protofibrillar and fibrillar forms.

However, the third hypothesis could describe α -synuclein as a completely harmless protein in fission yeast. This may be due to the differences in membrane composition between budding and fission yeast. If the membrane is slightly different in composition of phospholipids and glycolipids, α -synuclein's membrane binding properties may change (Davidson et. al., 1998).

Conclusions

Using budding and fission yeast models of Parkinson's

disease, we have inexpensively recreated a genetically flexible neuron to study protein misfolding and related toxicity. To study why dopaminergic degeneration is so specific, yeast serve as a good starting point to screen genes responsible for enhancing α -synuclein aggregation in response to oxidative stress. Although this system does not include compounds and substrates like dopamine or neuromelanin, we can genetically induce their effects, reactive oxygen species generation.

Yeast have conserved protein trafficking machinery and mitochondrial proteins that share similarities with humans, which allow us to study the effects of mitochondrial dysfunction on α -synuclein toxicity.

Evaluation of the two budding yeast mitochondrial mutants, *kgd1 Δ* and *glo4 Δ* , have shown us that α -synuclein isoforms and the mitochondria interact in various ways to produce PD in different ways. Studies with A76E- α -synuclein have elucidated the three keys to aggregation kinetics: charge, secondary structure, and hydrophobicity.

Limitations

Determining the phenotype of a fluorescence image is a subjective process that can be performed at different capacities at different times. For example, it is usually difficult to distinguish between an auto-fluorescing cell and a cell exhibiting a diffuse phenotype. The charged-coupled device on the camera finds the brightest pixel on the field of view and assigns that the highest numerical value for light intensity. So, if two objects were in the field of view and one was more brightly fluorescing, then the weakly fluorescing cell would be diminished even more. Thus, high variability in fluorescence within the sample will bring difficulty when assessing the fluorescence patterns.

Additionally, the limit of experiments available to analyze α -synuclein aggregates in *kgd1 Δ* . Since the aggregates seen in *kgd1 Δ* are novel due to their membrane-bound nature, it would be interesting to investigate the lipid content of these aggregates. More sophisticated techniques in molecular biology may be able to unravel the contents of these protein inclusions.

Future Directions

Four goals should be pursued in the future. First, it would be appropriate to evaluate the removal of the other citric acid cycle enzymes and test the effects of α -synuclein misfolding and toxicity. Second, the level of oxidative stress should be evaluated by measuring oxidatively modified proteins or using a DHR 123, a fluorescent detector of reactive oxygen species. Third, the A76E- α -synuclein experiments need to be repeated in order to statistically evaluate the novel localization properties found with this protein. Finally, toxicity should be defined by characterizing cell growth, cell death, and apoptosis with a chemical agent.

Acknowledgements

I would first like to thank Dr. Shubhik DebBurman for allowing me to choose a research topic independent of his current NIH grant goals. His gentle supervision over my project has permitted me to develop and design my own questions and experiments. I would also like to thank my thesis committee, Dr. Pliny Smith and Dr. Jill Van Newenhuizen, for providing valuable input to aid in the completion of my manuscript. Additionally, I am indebted to Dr. Ann Maine for pushing me to generate a

first draft during the fall semester of my senior year. Finally, I would like to recognize my laboratory colleagues for their friendship and moral support during the entire process: Katrina Brandis '06, Michael White '07, Mithaq Vahedi '08, Lokesh Kukreja '08, and Nengding Wang '09.

Note: Eukaryon is published by students at Lake Forest College, who are solely responsible for its content. The views expressed in Eukaryon do not necessarily reflect those of the College. Articles published within Eukaryon should not be cited in bibliographies. Material contained herein should be treated as personal communication and should be cited as such only with the consent of the author.

References

Abou-Sleiman PM, Muqit MM, Wood NW. Expanding insights of mitochondrial dysfunction in Parkinson's disease. *Nat Rev Neurosci*. 2006 Mar;7(3):207-19.

Adam-Vizi V. Production of reactive oxygen species in brain mitochondria: contribution by electron transport chain and non-electron transport chain sources. *Antioxid Redox Signal*. 2005 Sep-Oct;7(9-10):1140-9.

Bito A, Haider M, Briza P, Strasser P, Breitenbach M. Heterologous expression, purification, and kinetic comparison of the cytoplasmic and mitochondrial glyoxalase II enzymes, Glo2p and Glo4p, from *Saccharomyces cerevisiae*. *Protein Expr Purif*. 1999 Dec;17(3):456-64.

Bito A, Haider M, Hadler I, Breitenbach M. Identification and phenotypic analysis of two glyoxalase II encoding genes from *Saccharomyces cerevisiae*, GLO2 and GLO4, and intracellular localization of the corresponding proteins. *J Biol Chem*. 1997 Aug 22;272(34):21509-19. Erratum in: *J Biol Chem* 1997 Oct 31;272(44):28164.

Bonifati V, Rizzu P, Squitieri F, Krieger E, Vanacore N, van Swieten JC, Brice A, van Duijn CM, Oostra B, Meco G, Heutink P. DJ-1 (PARK7), a novel gene for autosomal recessive, early onset parkinsonism. *Neurol Sci*. 2003 Oct;24(3):159-60.

Brandis KA, Holmes IF, England SJ, Sharma N, Kukreja L, DebBurman SK. Alpha-Synuclein fission yeast model: concentration-dependent aggregation without plasma membrane localization or toxicity. *J Mol Neurosci*. 2006;28(2):179-91.

Brandis KA. Senior Thesis. Lake Forest College. 2006.

Caughey B, Lansbury PT. Protofibrils, pores, fibrils, and neurodegeneration: separating the responsible protein aggregates from the innocent bystanders. *Annu Rev Neurosci*. 2003;26:267-98. Epub 2003 Apr 9.

Chiti F, Stefani M, Taddei N, Ramponi G, Dobson CM. Rationalization of the effects of mutations on peptide and protein aggregation rates. *Nature*. 2003 Aug 14;424(6950):805-8.

Clark IE, Dodson MW, Jiang C, Cao JH, Huh JR, Seol JH, Yoo SJ, Hay BA, Guo M. *Drosophila pink1* is required for mitochondrial function and interacts genetically with parkin. *Nature*. 2006 Jun 29;441(7097):1162-6. Epub 2006 May 3.

Clayton DF, George JM. Synucleins in synaptic plasticity and neurodegenerative disorders. *J Neurosci Res*. 1999 Oct 1;58(1):120-9.

Conway KA, Harper JD, Lansbury PT. Accelerated in vitro fibril formation by a mutant alpha-synuclein linked to early-onset Parkinson disease. *Nat Med*. 1998 Nov;4(11):1318-20.

Conway KA, Rochet JC, Bieganski RM, Lansbury PT Jr. Kinetic stabilization of the alpha-synuclein protofibril by a dopamine-alpha-synuclein adduct. *Science*. 2001 Nov 9;294(5545):1346-9.

Cookson MR. The biochemistry of Parkinson's disease. *Annu Rev Biochem*. 2005;74:29-52.

Dauer W, Przedborski S. Parkinson's disease: mechanisms and models. *Neuron*. 2003 Sep 11;39(6):889-909.

Davidson WS, Jonas A, Clayton DF, George JM. Stabilization of alpha-synuclein secondary structure upon binding to synthetic membranes. *J Biol Chem*. 1998 Apr 17;273(16):9443-9.

de Arriba SG, Stuchbury G, Yarin J, Burnell J, Loske C, Munch G. Methylglyoxal impairs glucose metabolism and leads to energy depletion in neuronal cells-protection by carbonyl scavengers. *Neurobiol Aging*. 2006 Jun 14; [Epub ahead of print]

Davis L, Smith GR. Meiotic recombination and chromosome segregation in *Schizosaccharomyces pombe*. *Proc Natl Acad Sci U S A*. 2001 Jul 17;98(15):8395-402.

Dixon C, Mathias N, Zweig RM, Davis DA, Gross DS. alpha-Synuclein targets the plasma membrane via the secretory pathway and induces toxicity in yeast. *Genetics*. 2005 May;170(1):47-59. Epub 2005 Mar 2.

Drechsel DA, Liang LP, Patel M. 1-Methyl-4-phenylpyridinium-induced alterations of glutathione status in immortalized rat dopaminergic neurons. *Toxicol Appl Pharmacol*. 2007 Feb 12; [Epub ahead of print]

Eliezer D, Kutluay E, Bussell R Jr, Browne G. Conformational properties of alpha-synuclein in its free and lipid-associated states. *J Mol Biol*. 2001 Apr 6;307(4):1061-73.

Ellis RJ, Pinheiro TJ. Medicine: danger--misfolding proteins. *Nature*. 2002 Apr 4;416(6880):483-4.

Elsinga PH, Hatano K, Ishiwata K. PET tracers for imaging of the dopaminergic system. *Curr Med Chem*. 2006;13(18):2139-53.

Fantes P. and Beggs J. (2000). *The Yeast Nucleus* (Oxford Univ. Press, Oxford).

Funayama M, Hasegawa K, Kowa H, Saito M, Tsuji S, Obata F. A new locus for Parkinson's disease (PARK8) maps to chromosome 12p11.2-q13.1. *Ann Neurol*. 2002 Mar;51(3):296-301.

Galvin JE. Interaction of alpha-synuclein and dopamine metabolites in the pathogenesis of Parkinson's disease: a case for the selective vulnerability of the substantia nigra. *Acta Neuropathol (Berl)*. 2006 Aug;112(2):115-126. Epub 2006 Jun 22.

Gerlach M, Double KL, Ben-Shachar D, Zecca L, Youdim MB, Riederer P. Neuromelanin and its interaction with iron as a potential risk factor for dopaminergic neurodegeneration underlying Parkinson's disease. *Neurotox Res*. 2003;5(1-2):35-44.

Gibson GE, Blass JP, Beal MF, Bunik V. The alpha-ketoglutarate-dehydrogenase complex: a mediator between mitochondria and oxidative stress in neurodegeneration. *Mol Neurobiol*. 2005;31(1-3):43-63.

Gibson GE, Sheu KF, Blass JP, Baker A, Carlson KC, Harding B, Perrino P. Reduced activities of thiamine-dependent enzymes in the brains and peripheral tissues of patients with Alzheimer's disease. *Arch Neurol*. 1988 Aug;45(8):836-40.

Graham DG. Oxidative pathways for catecholamines in the genesis of neuromelanin and cytotoxic quinones. *Mol Pharmacol*. 1978 Jul;14(4):633-43.

Goedert M. Alpha-synuclein and neurodegenerative diseases. *Nat Rev Neurosci*. 2001 Jul;2(7):492-501.

Hofer A, Gasser T. New aspects of genetic contributions to Parkinson's disease. *J Mol Neurosci*. 2004;24(3):417-24.

Humphrey T. DNA damage and cell cycle control in *Schizosaccharomyces pombe*. *Mutat Res*. 2000 Jun 30;451(1-2):211-26.

Jensen PH, Nielsen MS, Jakes R, Dotti CG, Goedert M. Binding of alpha-synuclein to brain vesicles is abolished by familial Parkinson's disease mutation. *J Biol Chem*. 1998 Oct 9;273(41):26292-4.

Kahle PJ, Haass C, Kretschmar HA, Neumann M. Structure/function of alpha-synuclein in health and disease: rational development of animal models for Parkinson's and related diseases. *J Neurochem*. 2002 Aug;82(3):449-57.

Kessler JC, Rochet JC, Lansbury PT Jr. The N-terminal repeat domain of alpha-synuclein inhibits beta-sheet and amyloid fibril formation. *Biochemistry*. 2003 Jan 28;42(3):672-8.

Kitada T, Asakawa S, Hattori N, Matsumine H, Yamamura Y, Minoshima S, Yokochi M, Mizuno Y, Shimizu N. Mutations in the parkin gene cause autosomal recessive juvenile parkinsonism. *Nature*. 1998 Apr 9;392(6676):605-8.

Kruger R, Kuhn W, Leenders KL, Sprengelmeyer R, Muller T, Woitalla D, Portman AT, Maguire RP, Veenma L, Schroder U, Schols L, Epplen JT, Riess O, Przuntek H. Familial parkinsonism with synuclein pathology: clinical and PET studies of A30P mutation carriers. *Neurology*. 2001 May 22;56(10):1355-62.

Krobitsch S, Lindquist S. Aggregation of huntingtin in yeast varies with the length of the polyglutamine expansion and the expression of chaperone proteins. *Proc Natl Acad Sci U S A*. 2000 Feb 15;97(4):1589-94.

Kunst CB, Mezey E, Brownstein MJ, Patterson D. Mutations in SOD1 associated with amyotrophic lateral sclerosis cause novel protein interactions. *Nat Genet*. 1997 Jan;15(1):91-4.

- Langston JW, Ballard P, Tetrud JW, Irwin I. Chronic Parkinsonism in humans due to a product of meperidine-analog synthesis. *Science*. 1983 Feb 25;219(4587):979-80.
- Lashuel HA, Petre BM, Wall J, Simon M, Nowak RJ, Walz T, Lansbury PT Jr. Alpha-synuclein, especially the Parkinson's disease-associated mutants, forms pore-like annular and tubular protofibrils. *J Mol Biol*. 2002 Oct 4;322(5):1089-102.
- Lin MT, Beal MF. Mitochondrial dysfunction and oxidative stress in neurodegenerative diseases. *Nature*. 2006 Oct 19;443(7113):787-95.
- Ma J, Lindquist S. De novo generation of a PrPSc-like conformation in living cells. *Nat Cell Biol*. 1999 Oct;1(6):358-61.
- Masliah E, Rockenstein E, Adame A, Alford M, Crews L, Hashimoto M, Seubert P, Lee M, Goldstein J, Chilcote T, Games D, Schenk D. Effects of alpha-synuclein immunization in a mouse model of Parkinson's disease. *Neuron*. 2005 Jun 16;46(6):857-68.
- May BC, Govaerts C, Cohen FE. Developing therapeutics for the diseases of protein misfolding. *Neurology*. 2006 Jan 24;66(2 Suppl 1):S118-22.
- Muchowski PJ. Protein misfolding, amyloid formation, and neurodegeneration: a critical role for molecular chaperones? *Neuron*. 2002 Jul 3;35(1):9-12.
- Muchowski PJ, Schaffar G, Sittler A, Wanker EE, Hayer-Hartl MK, Hartl FU. Hsp70 and hsp40 chaperones can inhibit self-assembly of polyglutamine proteins into amyloid-like fibrils. *Proc Natl Acad Sci U S A*. 2000 Jul 5;97(14):7841-6.
- Outeiro TF, Lindquist S. Yeast cells provide insight into alpha-synuclein biology and pathobiology. *Science*. 2003 Dec 5;302(5651):1772-5.
- Outeiro TF, Muchowski PJ. Molecular genetics approaches in yeast to study amyloid diseases. *J Mol Neurosci*. 2004;23(1-2):49-60.
- Paisan-Ruiz C, Jain S, Evans EW, Gilks WP, Simon J, van der Brug M, Lopez de Munain A, Aparicio S, Gil AM, Khan N, Johnson J, Martinez JR, Nicholl D, Carrera IM, Pena AS, de Silva R, Lees A, Marti-Masso JF, Perez-Tur J, Wood NW, Singleton AB. Cloning of the gene containing mutations that cause PARK8-linked Parkinson's disease. *Neuron*. 2004 Nov 18;44(4):595-600.
- Park J, Lee SB, Lee S, Kim Y, Song S, Kim S, Bae E, Kim J, Shong M, Kim JM, Chung J. Mitochondrial dysfunction in Drosophila PINK1 mutants is complemented by parkin. *Nature*. 2006 Jun 29;441(7097):1157-61. Epub 2006 May 3.
- Pilcher H. Parkinson's vaccine on trial. *Lancet Neurol*. 2005 Aug;4(8):458-9.
- Sipiczki M. Where does fission yeast sit on the tree of life? *Genome Biol*. 2000;1(2):REVIEWS1011. Epub 2000 Aug 4.
- Sharma N, Brandis KA, Herrera SK, Johnson BE, Vaidya T, Shrestha R, Debburman SK. Alpha-Synuclein budding yeast model: toxicity enhanced by impaired proteasome and oxidative stress. *J Mol Neurosci*. 2006;28(2):161-78.
- Sharma N. Senior Thesis. Lake Forest College. 2004.
- Shoghi-Jadid K, Small GW, Agdeppa ED, Kepe V, Ercoli LM, Siddarth P, Read S, Satyamurthy N, Petric A, Huang SC, Barrio JR. Localization of neurofibrillary tangles and beta-amyloid plaques in the brains of living patients with Alzheimer disease. *Am J Geriatr Psychiatry*. 2002 Jan-Feb;10(1):24-35.
- Spillantini MG, Crowther RA, Jakes R, Hasegawa M, Goedert M. alpha-Synuclein in filamentous inclusions of Lewy bodies from Parkinson's disease and dementia with lewy bodies. *Proc Natl Acad Sci U S A*. 1998 May 26;95(11):6469-73.
- Starkov AA, Fiskum G, Chinopoulos C, Lorenzo BJ, Browne SE, Patel MS, Beal MF. Mitochondrial alpha-ketoglutarate dehydrogenase complex generates reactive oxygen species. *J Neurosci*. 2004 Sep 8;24(36):7779-88.
- Tatton WG, Chalmers-Redman R, Brown D, Tatton N. Apoptosis in Parkinson's disease: signals for neuronal degradation. *Ann Neurol*. 2003;53 Suppl 3:S61-70; discussion S70-2.
- Tretter L, Adam-Vizi V. Inhibition of alpha-ketoglutarate dehydrogenase due to H2O2-induced oxidative stress in nerve terminals. *Ann N Y Acad Sci*. 1999;893:412-6.
- Tretter L, Adam-Vizi V. Alpha-ketoglutarate dehydrogenase: a target and generator of oxidative stress. *Philos Trans R Soc Lond B Biol Sci*. 2005 Dec 29;360(1464):2335-45.
- Tretter L, Adam-Vizi V. Generation of reactive oxygen species in the reaction catalyzed by alpha-ketoglutarate dehydrogenase. *J Neurosci*. 2004 Sep 8;24(36):7771-8.
- Uversky VN, Fink AL. Amino acid determinants of alpha-synuclein aggregation: putting together pieces of the puzzle. *FEBS Lett*. 2002 Jul 3;522(1-3):9-13.
- Valente EM, Abou-Sleiman PM, Caputo V, Muqit MM, Harvey K, Gispert S, Ali Z, Del Turco D, Bentivoglio AR, Healy DG, Albanese A, Nussbaum R, Gonzalez-Maldonado R, Deller T, Salvi S, Cortelli P, Gilks WP, Latchman DS, Harvey RJ, Dallapiccola B, Auburger G, Wood NW. Hereditary early-onset Parkinson's disease caused by mutations in PINK1. *Science*. 2004 May 21;304(5674):1158-60. Epub 2004 Apr 15.
- Wang D, Qian L, Xiong H, Liu J, Neckameyer WS, Oldham S, Xia K, Wang J, Bodmer R, Zhang Z. Antioxidants protect PINK1-dependent dopaminergic neurons in Drosophila. *Proc Natl Acad Sci U S A*. 2006 Sep 5;103(36):13520-5. Epub 2006 Aug 24.
- Webster J, Urban C, Berbaum K, Loske C, Alpar A, Gartner U, de Arriba SG, Arendt T, Munch G. The carbonyl scavengers aminoguanidine and tenilsetam protect against the neurotoxic effects of methylglyoxal. *Neurotox Res*. 2005;7(1-2):95-101.
- Weinreb PH, Zhen W, Poon AW, Conway KA, Lansbury PT Jr. NACP, a protein implicated in Alzheimer's disease and learning, is natively unfolded. *Biochemistry*. 1996 Oct 29;35(43):13709-15.
- Wetzel R. For protein misassembly, it's the "I" decade. *Cell*. 1996 Sep 6;86(5):699-702.
- Whitehead RE, Ferrer JV, Javitch JA, Justice JB. Reaction of oxidized dopamine with endogenous cysteine residues in the human dopamine transporter. *J Neurochem*. 2001 Feb;76(4):1242-51.
- Wood SJ, Wypych J, Steavenson S, Louis JC, Citron M, Biere AL. alpha-synuclein fibrillogenesis is nucleation-dependent. Implications for the pathogenesis of Parkinson's disease. *J Biol Chem*. 1999 Jul 9;274(28):19509-12.
- Xu Y, Chen X. Glyoxalase II, a detoxifying enzyme of glycolysis byproduct methylglyoxal and a target of p63 and p73, is a pro-survival factor of the p53 family. *J Biol Chem*. 2006 Sep 8;281(36):26702-13. Epub 2006 Jul 10.
- Yang Y, Gehrke S, Imai Y, Huang Z, Ouyang Y, Wang JW, Yang L, Beal MF, Vogel H, Lu B. Mitochondrial pathology and muscle and dopaminergic neuron degeneration caused by inactivation of Drosophila Pink1 is rescued by Parkin. *Proc Natl Acad Sci U S A*. 2006 Jul 11;103(28):10793-8. Epub 2006 Jul 3.
- Zabrocki P, Pellens K, Vanhelmont T, Vandebroek T, Griffioen G, Wera S, Van Leuven F, Winderickx J. Characterization of alpha-synuclein aggregation and synergistic toxicity with protein tau in yeast. *FEBS J*. 2005 Mar;272(6):1386-400.
- Zarranz JJ, Alegre J, Gomez-Esteban JC, Lezcano E, Ros R, Ampuero I, Vidal L, Hoenicka J, Rodriguez O, Atares B, Llorens V, Gomez Tortosa E, del Ser T, Munoz DG, de Yébenes JG. The new mutation, E46K, of alpha-synuclein causes Parkinson and Lewy body dementia. *Ann Neurol*. 2004 Feb;55(2):164-73.
- Zecca L, Zucca FA, Albertini A, Rizzio E, Fariello RG. A proposed dual role of neuromelanin in the pathogenesis of Parkinson's disease. *Neurology*. 2006 Oct 10;67(7 Suppl 2):S8-11.
- Zimprich A, Biskup S, Leitner P, Lichtner P, Farrer M, Lincoln S, Kachergus J, Hulihan M, Uitti RJ, Calne DB, Stoessl AJ, Pfeiffer RF, Patenge N, Carbajal IC, Vieregge P, Asmus F, Muller-Mylhok B, Dickson DW, Meitinger T, Strom TM, Wszolek ZK, Gasser T. Mutations in LRRK2 cause autosomal-dominant parkinsonism with pleomorphic pathology. *Neuron*. 2004 Nov 18;44(4):601-7.